Thermo-economic study of waste heat recovery from condensing steam for hydrogen production by PEM electrolysis

Norbert Lümmen*, Assma Karouach, Stine Tveitan

Department of Mechanical and Marine Engineering, Western Norway University of Applied Sciences, Postboks 7030, 5020 Bergen, Norway

Abstract

The hydrogen production potential and cost from waste heat recovered from condensing steam in a combined heat and power facility has been calculated. Two different concepts for using the recovered energy by an organic Rankine cycle in PEM water electrolysis have been developed and compared. Thermo-economic analysis has been employed to calculate the exergetic unit cost of the produced hydrogen as function of ORC working fluid, steam condensing pressure and hours of available waste heat per year for a mass flow rate of 10 kg/s of condensing steam between 80 kPa and 200 kPa condenser pressure in the steam cycle. Hydrogen production rates in the range from 0.647 to 1.27 g H_2/kg steam were obtained. The exergetic unit cost of uncompressed, compressed (350 bar) and liquefied hydrogen were calculated. Costs as low as \$3.06/kg H_2 (uncompressed) could be achieved, when the use of waste heat was maximised. The lowest cost of compressed (350 bar) and liquefied hydrogen were \$4.11/kg H_2 and \$16.53/kg H_2, respectively. Depending on the chosen scenario, between 186 and 364 tonne hydrogen can be produced annually.

Highlights

- Two H_2 production concepts from waste heat and PEM electrolysis.
- All equations for organic Rankine cycle and thermo-economic analysis.
- Case study of H_2 production potential at combined heat and power plant.
- Compressed and liquid H_2 production cost calculation and comparison.

Keywords: waste heat recovery, organic Rankine cycle, hydrogen production, PEM electrolysis, thermo-economic analysis

*Corresponding author: Norbert Lümmen, nlu@hvl.no

1 Introduction

Hydrogen used as fuel has the potential to contribute to a reduction in greenhouse gas (GHG) emissions from the transport sector when it is produced from renewable forms of energy such as hydroelectricity. In Norway, the goal is to reduce the GHG emissions to 60% or less [1] than that of 1990's level, when 51.7 million tonne CO_2 equivalents were emitted, by the year 2030. From the current level of 53.3 million tonne CO_2 equivalents [2], a reduction by 22.3 million tonne is necessary over the next 12 years. In 2016, 16.4 million tonne CO_2 equivalents were emitted by the transport sector (road traffic, domestic aviation, navigation, fishing and motor equipment) [2]. By realising carbon emission free transport in Norway, about 74.3% of the necessary reductions to meet the national climate goals could be achieved by this sector alone. While electric passenger vehicles are considered to be the most suitable solution for private transport in passenger cars, hydrogen is favoured by the transport industry for long distance transport of heavy goods on land and at sea, where current and near future battery performance is insufficient for fully electric operation. The use of liquid hydrogen as fuel for passenger airplanes has been investigated as well [3]. With this broad application of hydrogen as fuel in the transport sector in mind, the future hydrogen needs, potential production facilities and logistic chains are currently under investigation. Due to the large hydropower resources in Norway, hydrogen does not need to be produced from Norway's natural gas resources, but can be produced renewably by means of electrolysis.

Following on from the use of primary energy for hydrogen production, the use of waste heat for the same objective is interesting and is worthy of consideration, as it may also contribute towards making other processes more energy efficient. Such a process is, for example, the combined heat and power plant (CHP) in Bergen, Western Norway, where the chemical energy of municipal solid waste is converted into electricity and district heat [4]. Due to the lower demand for district heat during the warmer period of the year, the facility rejects around 90 GWh of non-utilised process heat directly to the atmosphere between the months of May and August [5]. The aim of this article is to investigate, if this waste heat can be used to produce hydrogen at a cost that is economically feasible. It is then of interest to know if the production rate is large enough to supply a local customer from the transport sector with hydrogen.

The Bergen CHP plant consist of two parallel lines. Each line has its own combustion chamber, heat exchanger to the steam cycle, pump, steam turbine and heat exchanger (condenser) to either the district heat network or atmosphere. One of these steam cycles has a turbine outlet pressure of 80 kPa at a mass flow rate of slightly more than 10 kg/s [5]. Yilmaz et al. recently investigated the cost of hydrogen production in a combined flash-binary geothermal power plant [6]. In their study, the latent energy of the steam fraction of the flashed geothermal water at 200 kPa was used to supply an organic Rankine cycle (ORC) with energy. The electricity produced by means of the ORC was used to power a PEM electrolyser to hydrogen production from water.

In this article, however, the energy source for the ORC is the latent heat of the condensing steam from one of the CHP facility's steam cycle. This energy would normally be transferred to the atmosphere, when not utilised as district heat. As the waste heat is only available for hydrogen production for a certain period of the year, auxiliary electric power is used to run the electrolysis and other equipment for the remainder of the annual operation time of 8000 hours. This duration is equal to the operation

time of the CHP plant. It is therefore the maximum amount of time with waste heat availability. The maximum annual operation time for hydrogen production is thus also set to the same duration.

Thermo-economic analysis is used for estimating the production cost of the hydrogen as produced by the electrolyser and for both compressed and liquefied hydrogen. Production rate and cost are studied as a function of ORC working fluid, steam condensing pressure and hours of waste heat use during a year of operation for 20 years of plant lifetime. As different ORC-fluids behave differently at given conditions, it was important to ascertain, which ORC-fluid gave the maximum output power and consequently the largest hydrogen production potential. The pressure of the condensing steam defines its temperature and thereby the maximum temperature in the organic Rankine cycle. This has an impact on the maximum thermal efficiency of the ORC-unit. The chosen pressure range was based on typical turbine outlet temperatures, which may be followed by heat exchangers to a district heat network, where the latter is operated only during the colder part of the year. As the demand for district heat changes with the seasons, weather and geographical location of the plant, the availability of waste heat for recovery changes as well and may vary from a few hundred to several thousand hours.

Hydrogen production by electrolysis based on utilising low temperature heat has been studied by Sigurvinsson et al. [7] for geothermal springs in Iceland. Using geothermal water at 160°C as a heat source for an organic Rankine cycle (ORC) and preheating the electrolysis water for polymer electrolyte membrane (PEM) electrolysis powered by ORC-generated electricity was studied by Yilmaz and Kanoglu in a thermodynamic analysis [8], followed by a thermo-economic analysis by Yilmaz et al. for the same setup [9]. A production rate 0.34 g H_2 per kilogram of geothermal water was found along with energy and exergy efficiencies of 6.7% and 23.8% respectively. The exergetic cost of hydrogen production was \$2.37/kg H_2 for hydrogen coming directly from the electrolysing process (subsequent compression or liquefaction was not considered). In a further study by Yilmaz et al. [6], the geothermal water was flashed from 1.56 MPa and 200°C to 600 kPa. The steam fraction was expanded in its own turbine while the condensate fraction supplied an ORC with heat. The combined turbine output power (\$0.04/kWh) was used to run a PEM electrolysis unit. A production rate of 0.0498 kg H_2 per kg geothermal water at an exergetic unit cost of \$3.14/kg H_2 and an exergy efficiency of 45.8% of the overall system could theoretically be achieved. This cost is a typical value for hydrogen produced by electrolysis according to Dincer and Acar [10].

Nami et al. [11] studied the production of hydrogen by PEM analysis with waste heat recovered from a gas turbine cycle with helium as gas turbine working fluid by means of two organic Rankine cycles. Under the optimised conditions, the exergy efficiency and rate of produced hydrogen were 49.2% and 56.2 kg/h, respectively. Organic Rankine cycles are also suitable for hydrogen production by electrolysis with concentrated solar energy as an energy source, which is used to evaporate the working fluid as studied by Shahin et al. [12] or Yüksel [13]. Ferrero & Santarelli recently investigated a high pressure and temperature PEM-water electrolyser integrated with multi-junction solar cells, which showed higher system efficiency compared with separate photovoltaic electricity generation and hydrogen production by electrolysis [14]. Cao et al. conducted exergy analysis and optimisation of a combined cooling and power system driven by geothermal energy (mass flow rate of 30 kg/s) for ice-making and hydrogen production by alkaline electrolysis (0.074 g H_2/kg geothermal fluid) [15]. The second law efficiency of hydrogen production was approximately 18.3%.

The development of water electrolysis cost and performance was analysed by Schmidt et al. for both alkaline, PEM and solid oxide electrolysis cell (SOEC) systems [16]. It was reported that capital cost reductions of up to 24% are possible, where production scale up of electrolysing equipment alone can stand for 17-30% of these reductions. The lifetime of the equipment can possibly be extended to between 60,000 and 90,000 hours. Of the three main methods, both alkaline and PEM electrolysis are usually carried out at temperatures below 100°C. Compared with alkaline systems, PEM systems are still less mature and more expensive, but have the advantage of a higher power density and cell efficiency. According to Schmidt et al. [16] the trend will go from alkaline systems to PEM based systems before 2030. Therefore, PEM electrolysis was considered as hydrogen production method in this work.

The current work investigates low temperature waste heat as energy source for hydrogen production by PEM electrolysis. The temperature of the condensing steam is even lower than that of the geothermal water used by Yilmaz and Kanoglu [8]. It lies in a range typical for waste heat from CHP plants, where the waste heat is normally used for district heating for most parts of the year, but might be rejected to the surroundings at low or no demand for district heat. The intermittent nature of the availability of waste heat is in contrast with constantly available sources such as geothermal heat sources studied by Yilmaz and Kanoglu [8] or Sigurvinsson et al. [7]. The fraction of the maximum annual operating time, where energy can be recovered from waste as electricity, will have an impact on the cost of electricity generation. It is of interest to find out how the cost of hydrogen production varies with the amount of time waste heat is available for energy recovery for this purpose and what the production cost is, when electricity from the grid is employed in order to use the hydrogen production equipment for the full annual operational time of 8000 hours. To the authors' knowledge, this mixed use of recovered and primary energy for hydrogen production has not previously been investigated in a thermo-economic analysis of hydrogen production.

The following work is structured as follows. In Section 2, the different hydrogen production concepts are introduced. The necessary equations for the organic Rankine cycle, the electrolysis, the energy need and efficiency for hydrogen compression to 350 bar as well as liquefaction, the hydrogen production efficiency and the thermo-economic analysis are presented. Results are presented in Section 3 and discussed in Section 4. Finally, conclusions are drawn in Section 5.

2 Method

Waste heat recovery by means of an organic Rankine cycle with subsequent production of hydrogen by PEM-electrolysis with electricity produced from the ORC-power output has been investigated by means of energy, exergy and thermo-economic analysis. Different ORC-working fluids were compared with respect to ORC-power output. The waste heat recovery and hydrogen production facility is fictive while the waste heat source is condensing steam in an existing combined heat and power facility in Bergen, Norway.

The ORC-model used in the calculations of extractable energy from the steam leaving the turbine is a further development of the simple subcritical ORC-model with a single non-condensing heat source used by Lümmen et al. [17]. In order to be applicable to waste heat fluids, that undergo a phase

transition, some of the equations for the simple ORC (see [17]) had to be modified. The full set of equations is presented in the following sections.

2.1 Concepts for hydrogen production from recovered waste heat

Two different concepts for hydrogen production with waste steam are considered. Both are based on the simple subcritical ORC without regeneration.

A: All electricity generated by means of the ORC is used for electrolysis of water; auxiliary heat is used for preheating the electrolysis water and for the compression or liquefaction of the produced hydrogen (Figure 1).

B: The electricity generated by means of the ORC is used for both electrolysis and compression or liquefaction of the hydrogen produced; auxiliary heat is used for preheating of the electrolysis water (Figure 2).

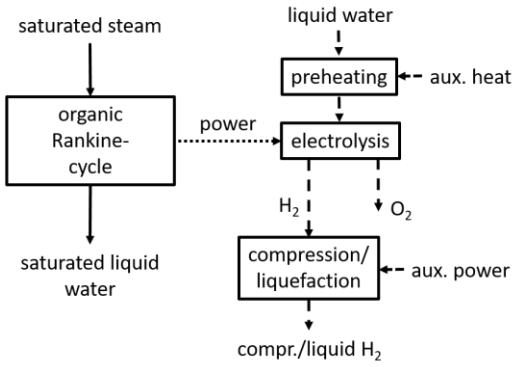

Figure 1. Concept A with auxiliary heat for preheating and auxiliary power for compression or liquefaction of the produced hydrogen.

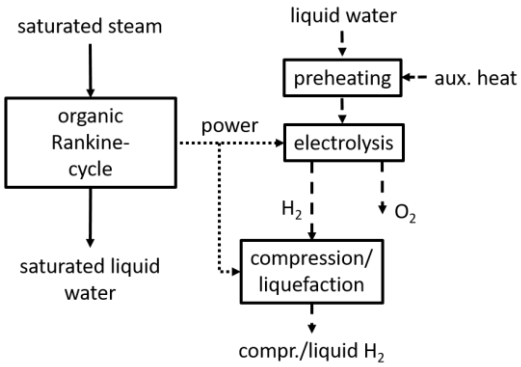

Figure 2. Concept B with auxiliary heat for preheating while electric power generated by the ORC is used for both electrolysis and compression or liquefaction.

2.2 Basic equations for both concepts

Steam coming from the exit of a steam turbine (state 6 in Figure 3 and Figure 4) is assumed as a heat source for the ORC. The steam is either superheated or can be characterised by its quality at the outlet pressure. This pressure is assumed constant during the entire heat exchanging process with the ORC working fluid. The same is done for the heat sink fluid, which is treated like incompressible liquid water with a temperature of 10°C at the inlet to the condenser (state 11 in Figure 3 and Figure 4). A specific heat capacity at constant pressure of 4.18 kJ/(kg·°C) is used. In general, pressure losses in all fluids are neglected during the heat exchange processes. In the organic Rankine cycle, the same maximum pressure is used in all states between the outlet of the pump (state 4) and the inlet of the turbine (state 1) and the same minimum pressure is applied in all states between the turbine outlet (state 2) and the pump inlet (state 3).

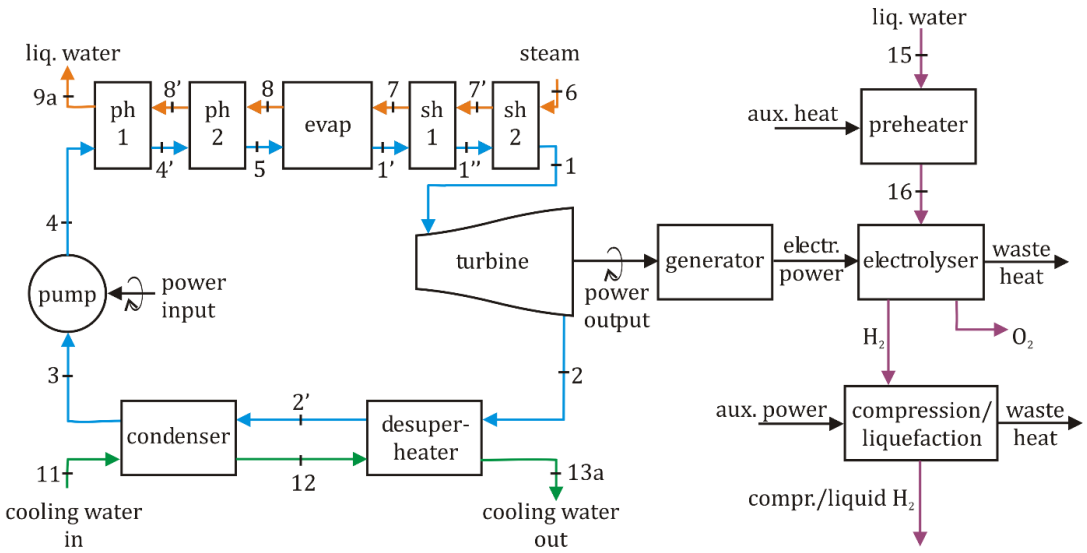

Figure 3. Simple subcritical ORC with a single condensing waste heat fluid and heat sink. For the calculations in the model, two preheaters (ph) and two superheaters (sh) are necessary.

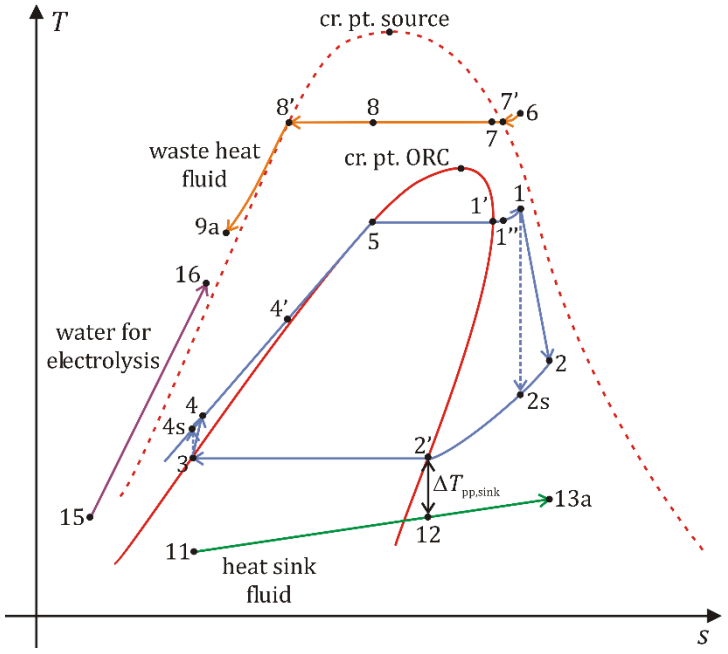

Figure 4. T-s-diagram for the simple subcritical ORC with a condensing waste head fluid. The abbreviation 'cr. pt.' stands for 'critical point'.

The following equations are used in the calculation of state properties in the different fluids. Based on the ORC-working fluid properties in state 1 (turbine inlet, see Figure 3 and Figure 4), the specific enthalpy in state 2 (turbine outlet) is calculated by

$$h_2 = h_1 - \eta_{s,\text{turbine}}(h_1 - h_{2s}) \tag{1}$$

where h_{2s} is the specific enthalpy in case of isentropic expansion between the pressures in states 1 and 2 and $\eta_{s,\text{turbine}}$ is the isentropic efficiency of the turbine.

It is assumed that the ORC-working fluid is in the saturated liquid phase at the inlet of the pump, which is at $P_{\min}$. The specific enthalpy at the pumps outlet is

$$h_4 = h_3 + \frac{(h_{4s} - h_3)}{\eta_{s,\text{pump}}} \tag{2}$$

where h_{4s} is the enthalpy at the pump outlet for isentropic pressure increase and $\eta_{s,\text{pump}}$ is the pump's isentropic efficiency.

The working fluid reaches its saturated liquid phase in state 5. The saturated vapour phase is designated state no. 1'.

The mass flow rate $\dot{m}_{\text{ORC}}$ of the working fluid is calculated by

$$\dot{m}_{\text{ORC}} = \varepsilon_{\text{evap}} \dot{m}_{\text{source}} \frac{(h_6 - h_{9\text{a}})}{(h_1 - h_4)} \tag{3}$$

where $\varepsilon_{\text{evap}}$ is the effectiveness of the heat exchanging process and $\dot{m}_{\text{source}}$ the mass flow rate of the waste heat fluid. The heat sink fluid is assumed to be in a single phase with specific heat capacity at constant pressure $c_{P,\text{sink}}$. The corresponding mass flow rate of the heat sink fluid $\dot{m}_{\text{sink}}$ undergoing a limited maximum temperature increase of $\Delta T_{\text{heat sink,max}}$ obtained by

$$\dot{m}_{\text{sink}} = \dot{m}_{\text{ORC}} \frac{(h_2 - h_3)}{\varepsilon_{\text{cond}} c_{P,\text{sink}} \Delta T_{\text{heat sink,max}}} \tag{4}$$

with the heat exchanger (condenser) effectiveness $\varepsilon_{\text{cond}}$. Note, that the actual increase in the heat sink temperature will only be equal to $\Delta T_{\text{heat sink,act}} = \varepsilon_{\text{cond}} \Delta T_{\text{heat sink,max}}$.

Dividing the heat exchange processes into several subprocesses helps in evaluating solutions obtained and errors encountered when using the built-in solver in Microsoft Excel. It makes the drawing of a simple T-s-diagram possible in this software. Furthermore, it allows for easier calculation of heat exchange surface index as defined by Branchini et al. [18], which take the logarithmic mean temperature differences of each subprocess into account. In the thermo-economic analysis (Section 2.8), only a single heat exchanger is assumed for each ORC working fluid evaporation and condensing.

Under the assumption that the pressure is constant in both steam and ORC working fluid during heat exchange, the enthalpy in the various states is calculated as follows

$$h_8 = h_9 + \frac{\dot{m}_{\text{ORC}}}{\dot{m}_{\text{source}}} (h_5 - h_4) \tag{5}$$

and

$$h_7 = h_8 + \frac{\dot{m}_{\text{ORC}}}{\dot{m}_{\text{source}}} (h_{1'} - h_5) \tag{6}$$

In a similar way, the specific enthalpies in states 4' and 1'' are calculated

$$h_{4'} = h_4 + \frac{\dot{m}_{\text{source}}}{\dot{m}_{\text{ORC}}} (h_{8'} - h_{9a}) \tag{7}$$

and

$$h_{1,,} = h_1 - \frac{\dot{m}_{\text{source}}}{\dot{m}_{\text{ORC}}}(h_6 - h_{7,}) \tag{8}$$

The heat sink fluid enters the low temperature side of the working-fluid-condenser at $P_{\text{sink}} = P_{11}$ and $T_{\text{min,sink}} = T_{11}$. At the pinch point with the working fluid, the temperature has increased to

$$T_{12} = T_{2,} - \Delta T_{\text{pp,sink,min}} \tag{9}$$

where $\Delta T_{\text{pp,sink,min}}$ is the desired minimum pinch point temperature difference between ORC working fluid and heat sink fluid. The heat sink fluid temperature at the outlet of the condenser is

$$T_{13a} = T_{12} + \frac{\dot{m}_{\text{ORC}}(h_2 - h_{2,})}{\dot{m}_{\text{sink}} c_{P,\text{sink}}} \tag{10}$$

The maximum available heat transfer rate from heat source to working fluid is

$$\dot{Q}_{\text{source}} = \dot{m}_{\text{source}}(h_6 - h_{9\text{a}}) \tag{11}$$

The recovered exergy rate is equal to the net work output from the ORC and given by

$$\dot{X}_{\text{recovered}} = \dot{W}_{\text{ORC,net,out}} = \dot{m}_{\text{ORC}}[(h_1 - h_2) - (h_4 - h_3)] \tag{12}$$

where the first specific enthalpy difference on the right hand side is the specific work output from the turbine and the second specific enthalpy difference is the specific work input to the pump.

The available electric power generated from the recovered waste heat by the organic Rankine cycle is calculated by

$$\dot{W}_{\text{el}} = \eta_{\text{gen}}\, \dot{W}_{\text{ORC,net,out}} \tag{13}$$

The generator efficiency η_{gen} is set to 95 %.

The heat rejection rate from the working fluid in the condenser is

$$\dot{Q}_{\text{sink}} = \dot{m}_{\text{ORC}}(h_2 - h_3) \tag{14}$$

The total available exergy rate of heat source fluid is given by

$$\dot{X}_{\text{source,total}} = \dot{m}_{\text{source}}[(h_6 - h_0) - T_0(s_6 - s_0)] \tag{15}$$

where changes in kinetic end potential energy of the steam are neglected. The available exergy for recovery by the ORC is limited by the final state of the condensing waste heat fluid (state 9a), which has to be specified. It is therefore given by the exergy rate change of the heat source fluid between states 6 and 9a

$$\dot{X}_{\text{source,available}} = \dot{m}_{\text{source}}[(h_6 - h_{9a}) - T_0(s_6 - s_{9a})] \tag{16}$$

where changes in kinetic and potential energy of the waste heat fluid have been neglected once more.

The thermal efficiency of the ORC is defined as

$$\eta_{\text{th}} = \frac{\dot{W}_{\text{ORC,net,out}}}{\dot{Q}_{\text{source}}} \tag{17}$$

Two different definitions of the second law efficiency of the organic Rankine cycle are used, based on the respective exergy supply rates

$$\eta_{\text{II,ORC,total}} = \frac{\dot{W}_{\text{ORC,net,out}}}{\dot{X}_{\text{source,total}}} \tag{18}$$

and

$$\eta_{\text{II,ORC,available}} = \frac{\dot{W}_{\text{ORC,net,out}}}{\dot{X}_{\text{source,available}}} \tag{19}$$

The values of $\eta_{\text{II,ORC,available}}$ are larger than those of $\eta_{\text{II,ORC,total}}$, because the available exergy rate is smaller than the total exergy rate at the same net power output (recovered exergy).

2.3 Selection of working fluids

Several working fluids are available for waste heat recovery to electricity by ORCs. Ref. [19] gives an overview over a number of different relevant publications and the working fluids used by their authors. For this study, a selection of different fluids was chosen where the criteria were low global warming potential (GWP), low ozone depletion potential (ODP), low flammability and flame propagation; according to the ASHRAE classification (either 1 or 2L) [20]. Current regulation by the European Union (EU) sets an upper limit on GWP for most applications of refrigerants to 150 from year 2022 on [21]. With respect to health and safety, low toxicity is preferable (A in the ASHRAE classification as opposed to B, which stands for higher toxicity).

The choice fell onto the three hydrofluorolefines (HFO) R1234ze(Z), R1234ze(E), and R1234yf (all ASHRAE class A2L) and the hydrochlorofluoroolefine (HCFO) R1233zd(E), which has ASHRAE class A1. R717 (ammonia) was part of the studied fluids as well due to having zero GWP and ODP. It is a working fluid often used in industrial and residential heat pump applications even though it is in the higher toxicity class (B) within the ASHRAE-scheme. It has a much higher critical pressure compared with the other fluids, but with a critical temperature similar to that of the R1234ze-variants. Both ethanol and R717 have a 'wet' vapour part of the saturation curve (negative slope), while the aforementioned fluids have a 'dry' saturation curve. Isobutane (R600a) was included in the list as well as it was the ORC working fluid employed in the work of Yilmaz [22].

2.4 Electrolysis

The calculation of the hydrogen production rate is based on the model published by Ni et al. [23], where all necessary equations and values can be found. The model is applied in the following way: At first, a target current density J is chosen for the electrolyser. It is set to $J = J_{\text{target}} = 5\ \text{kA/m}^2$ in this work. This is a trade-off between efficiency (lower current density is better) [23] and cost (higher current density needs less membrane area) [24]. Afterwards, the activation overpotentials for anode ($\eta_{\text{act,a}}$) and cathode ($\eta_{\text{act,c}}$) and the ohmic overpotential (η_{ohm}) are calculated. The reversible potential is

$$V_0 = \frac{\Delta \bar{G}(T,P)}{nF} \tag{20}$$

where n is the number of electrons (2) in the electrolysis reaction, F the Faraday constant and $\Delta \bar{G}(T,P)$ the change in molar Gibbs energy during the electrolysis reaction. The latter depends on temperature T and pressure P and can be calculated following the procedure used in ref. [25] with data from NASA Technical Memorandum 4513 [26]. The cell potential V is the sum of the reversible potential, the activation overpotentials and the ohmic overpotential

$$V = V_0 + \eta_{\text{act,a}} + \eta_{\text{act,c}} + \eta_{\text{ohm}} \tag{21}$$

It is used to calculate the electric power density $e_{\text{el}} = JV$, which in turn is used to calculate the necessary membrane area A

$$A = \frac{\dot{W}_{\text{el}}}{e_{\text{el}}} \tag{22}$$

Finally, the hydrogen production rate can be calculated with

$$\dot{N}_{\text{H}_2} = \frac{JA}{2F} \tag{23}$$

with units of amount of substance per unit of time or with $\dot{m}_{\text{H}_2} = M_{\text{H}_2}\dot{N}_{\text{H}_2}$ with units of mass of hydrogen per unit of time; where M_{H_2} is the molar mass of hydrogen.

The necessary mass flow of water into the electrolyser is based on the mass balance and the ratio of the mole masses between hydrogen and water

$$\dot{m}_{\text{H}_2\text{O}} = \dot{m}_{\text{H}_2} \frac{M_{\text{H}_2\text{O}}}{M_{\text{H}_2}} \tag{24}$$

The following amount of heat must be supplied in order to preheat the water from the surroundings temperature to the electrolysis temperature and at constant pressure

$$\dot{Q}_{\text{preheat}} = \dot{m}_{\text{H}_2\text{O}} \left(h\left(T_{\text{electrolysis}}, P_0\right) - h(T_0, P_0) \right)_{\text{H}_2\text{O}} \tag{25}$$

The electrolysis process needs to be kept at constant temperature. The following equation can be used to calculate if either heating or cooling of the electrolysis process is necessary [23]

$$\dot{Q}_{\text{PEM,process}} = \frac{J}{2F} \left(T\Delta S - 2F\left(\eta_{\text{act,a}} + \eta_{\text{act,c}} + \eta_{\text{ohm}}\right) \right) \tag{26}$$

In this equation, T is the temperature of the electrolysis process and ΔS the corresponding molar entropy change. If $\dot{Q}_{\text{PEM,process}} < 0$, heat needs to be rejected, while heat needs to be supplied to the electrolyser when $\dot{Q}_{\text{PEM,process}} > 0$. At the chosen values of J and T, heat needs to be rejected (to the surroundings) in the order of a few kilowatt because the heat generated during the electrolysis process due to irreversibilities exceeds the heat necessary for the reaction [23].

2.5 Hydrogen compression

The necessary energy for compression of the produced hydrogen to 350 bar is calculated. Although passenger cars use hydrogen compressed to 700 bar due to the stronger space constraints regarding hydrogen storage tanks, truck vehicles in a similar manner to hydrogen-electric waste collection vehicles [27] use compressed hydrogen at 350 bar. The calculation of the required compression power $\dot{W}_{\text{act, compr.}}$ is based on an isothermal compression process from 1 bar to 350 bar with 78% isothermal efficiency.

$$\dot{W}_{\text{act, compr.}} = \eta_T \dot{m}_{\text{H}_2} RT \ln \frac{P_{\text{final}}}{P_{\text{initial}}} \tag{27}$$

2.6 Hydrogen liquefaction

The reversible work for liquefying a kilogram of hydrogen from its state leaving the electrolyser at pressure P_0 and temperature $T_{\text{electrolysis}}$ to the saturated liquid state (quality $x = 0$) at the same pressure is

$$w_{\text{rev,liq.}} = \left(h\left(T_{\text{electrolysis}}, P_0\right) - h(x = 0, P_0)\right) - T_0 \left(s\left(T_{\text{electrolysis}}, P_0\right) - s(x = 0, P_0)\right) \tag{28}$$

and can be obtained with CoolProp [28]. The actual specific electrolysis work can be calculated if, for example, the second law efficiency $\eta_{\text{II,liq.}}$ of the liquefaction process is known.

$$w_{\text{act,liq.}} = \frac{w_{\text{rev,liq.}}}{\eta_{\text{II,liq.}}} \tag{29}$$

Hammad and Dincer investigated an advanced system for hydrogen liquefaction and provided its second law efficiency as a function of hydrogen mass flow [29]. The functional relationship has been approximated with the following function with data points taken from a figure in ref. [29].

$$\eta_{\text{II,liq.}}\left(\dot{m}_{\text{H}_2}\right) = a \exp\left(-b \cdot \dot{m}_{\text{H}_2}\right) + c \tag{30}$$

with a = 0.0920, b = 0.835 s/kg H_2 and c = 0.0402. The data points in ref. [29] ranged from 0.05 kg/s to 2.0 kg/s, while the hydrogen mass flow is lower in this work. The values of $\eta_{\text{II,liq.}}$ used in this work are therefore extrapolated from the data in ref. [29] and lies between 13.1% and 13.2% for mass flow rates between 0.0065 kg/s and 0.013 kg/s.

Thus, the actual power necessary for the liquefaction of the produced hydrogen is

$$\dot{W}_{\text{act, liq.}} = \dot{m}_{\text{H}_2} w_{\text{act,liq.}} \tag{31}$$

2.7 Additional equations for concept B

In contrast to concept A, all electricity generated by the ORC-unit is used for both electrolysis and either H_2 compression or liquefaction and the use of auxiliary electricity is avoided during the use of waste heat (see Figure 2). When the power $\dot{W}_{\text{el}}$ produced by the generator with efficiency η_{gen} is used to supply both the electrolyser and the compression/liquefaction system (see Figure 2), the problem solver in Microsoft Excel can be used to find a solution. This approach is necessary because the available electric power defines the possible hydrogen production rate, on which the actual compression or liquefaction power ($\dot{W}_{\text{act,compr./liq.}}$) depends; namely,

$$\dot{W}_{\text{el}} = \eta_{\text{gen}}\, \dot{W}_{\text{ORC,net,out}} = \dot{W}_{\text{electrolysis}} + \dot{W}_{\text{act,compr./liq.}} \tag{32}$$

The factor z_{el} is introduced in order to express the electrolysis power $\dot{W}_{\text{electrolysis}}$ as a fraction of the available electric power

$$\dot{W}_{\text{electrolysis}} = z_{\text{el}} \dot{W}_{\text{el}} \tag{33}$$

The problem solver (see Section 2.10) can then be used to find the correct value of z_{el} such that the sum of the electrolysis power and the corresponding actual compression/liquefaction power are equal to the available electric power.

2.8 Efficiency of H_2 production

The energy efficiency (1st law efficiency) of the hydrogen production process can be defined based on the higher heating value of hydrogen and the amount of hydrogen produced by means of the available energy in the condensing steam and the other energy inputs. The energy efficiency for concept A is then

$$\eta_{\text{I,H}_2\text{,HHV,A,compr./liq.}} = \frac{\dot{m}_{\text{H}_2} \text{HHV}_{\text{H}_2}}{\dot{Q}_{\text{source}} + \dot{Q}_{\text{preheat}} + \dot{W}_{\text{act, compr./liq.}}} \tag{34}$$

with a HHV_{H_2} value of 141 800 kJ/kg H_2. Similarly, the same can be done based on the lower heating value (LHV_{H_2} = 120 000 kJ/kg H_2). In the case where process heat has to be supplied to the electrolyser ($\dot{Q}_{\text{PEM,process}} > 0$), this contribution has to be added in the denominator of equation (34).

For concept B, the compression/liquefaction power is not an external input but generated from $\dot{Q}_{\text{source}}$. Therefore, the energy efficiency is in this case

$$\eta_{\text{I,H}_2\text{,HHV,B, compr./liq.}} = \frac{\dot{m}_{\text{H}_2} \text{HHV}_{\text{H}_2}}{\dot{Q}_{\text{source}} + \dot{Q}_{\text{preheat}}} \tag{35}$$

Again, in the case where process heat has to be supplied to the electrolyser, this contribution has to be added in the denominator of equation (35).

The second law efficiencies are defined accordingly. The specific exergy of the produced hydrogen is the sum of the physical (or thermal) exergy and the chemical exergy ($ex_{\text{chem,H}_2} = 11711.31$ kJ/kg [30]). It may be related to either power input to the electrolyser, the necessary exergy for preheating the electrolysis water $\dot{X}_{\dot{Q}_{\text{preheat}}}$ and the actual power for either compression or liquefaction $\dot{W}_{\text{act,compr./liq.}}$.

$$\eta_{\text{II,H}_2\text{,A,compr./liq.,1}} = \frac{\dot{m}_{\text{H}_2} \psi_{\text{H}_2}^{\text{ph.+chem.}}}{\dot{W}_{\text{electrolysis}} + \dot{X}_{\dot{Q}_{\text{preheat}}} + \dot{W}_{\text{act,compr./liq.}}} \tag{36}$$

Instead of the electrolysis power, the rate of change of thermal exergy $\dot{m}_{\text{source}} \Delta\psi_{\text{source}}$ of the condensing steam may be used, giving a broader picture of the exergy recovery from what is considered the waste heat source. In this case, the second law efficiency of concept A becomes

$$\eta_{\mathrm{II,H_2,A,compr./liq.,2}} = \frac{\dot{m}_{\mathrm{H_2}} \psi_{\mathrm{H_2}}^{\mathrm{ph.+chem.}}}{\dot{m}_{\mathrm{source}} \Delta\psi_{\mathrm{source}} + \dot{X}_{\dot{Q}_{\mathrm{preheat}}} + \dot{W}_{\mathrm{act,compr./liq.}}} \tag{37}$$

In order to calculate the exergy rate of the preheating power a heat source temperature is needed. A constant heat source temperature of at least 5°C more than the electrolysis temperature is assumed. The values of the second law efficiency are even lower than the first law efficiency and only a few percent.

The second law efficiency for concept B is written accordingly as either

$$\eta_{\mathrm{II,H_2,B,compr./liq.,1}} = \frac{\dot{m}_{\mathrm{H_2}} \psi_{\mathrm{H_2}}^{\mathrm{ph.+chem.}}}{\dot{W}_{\mathrm{el}} + \dot{X}_{\dot{Q}_{\mathrm{preheat}}}} \tag{38}$$

as both electrolysis and compression/liquefaction are supplied from the same source of electricity, or

$$\eta_{\mathrm{II,H_2,B,compr./liq.,2}} = \frac{\dot{m}_{\mathrm{H_2}} \psi_{\mathrm{H_2}}^{\mathrm{ph.+chem.}}}{\dot{m}_{\mathrm{source}} \Delta\psi_{\mathrm{source}} + \dot{X}_{\dot{Q}_{\mathrm{preheat}}}} \tag{39}$$

2.9 Equations for the thermo-economic analysis

2.9.1 Basic equations

The main equations for the thermo-economic analysis were taken from the works of Uysal et al. [31], Lazzaretto and Tsatsaronis [32] and Bejan et al. [33]. In order to calculate the cost of a kilogram of hydrogen, the cost rates not only of material and energy streams, but also the levelised capital investment cost rates $\dot{Z}$ of the involved equipment need to be calculated. For this, the so called hourly levelised cost method is used [31, 33]. The present worth factor (PWF) and capital recovery factor (CRF) are defined as

$$\mathrm{PWF} = \frac{1}{(1+i)^n} \tag{40}$$

$$\mathrm{CRF} = \frac{i(1+i)^n}{(1+i)^n - 1} \tag{41}$$

where i is the interest rate and n the lifetime of the facility in years. The salvage value (SV) is given as a fraction (μ) of the total capital investment (TCI)

$$\mathrm{SV} = \mu \cdot \mathrm{TCI} \tag{42}$$

The present worth (PW) of the facility is calculated by

$$\mathrm{PW} = \mathrm{TCI} - \mathrm{SV} \cdot \mathrm{PWF} \tag{43}$$

The present worth is used to determine the annual capital cost (AC) by multiplying the capital recovery factor with the present worth

$$\mathrm{AC} = \mathrm{CRF} \cdot \mathrm{PW} = \mathrm{CRF} \cdot \mathrm{TCI}\left(1 - \frac{\mu}{(1+i)^n}\right) \tag{44}$$

According to Bejan et al. [33], the total capital investment for a new facility can be estimated based on the total purchased equipment cost ($\mathrm{PEC}_{\mathrm{total}}$) by

$$\mathrm{TCI} = 6.32 \cdot \mathrm{PEC}_{\mathrm{total}} \tag{45}$$

while a factor of 4.16 is used if an existing facility is extended.

The annual capital investment cost rate of the whole system is then given by

$$\dot{Z}_{\mathrm{system}}^{\mathrm{total}} = \mathrm{AC} \cdot \frac{\phi}{\tau} \tag{46}$$

where ϕ is the maintenance factor and τ is the number of hours per year that the system is in operation. The total purchased equipment cost of a system consisting of N components is calculated by

$$\mathrm{PEC}_{\mathrm{total}} = \sum_{k=1}^{N} \mathrm{PEC}_k \tag{47}$$

The levelised purchased equipment cost of a component k is then

$$\mathrm{PEC}_k^* = \mathrm{PEC}_k \cdot \frac{\mathrm{PEC}_{\mathrm{total}}}{\mathrm{TCI}} = \frac{\mathrm{PEC}_k}{6.32} \tag{48}$$

for a new system. The levelised capital investment cost rate of a component k is determined by

$$\dot{Z}_k^{\mathrm{total}} = \dot{Z}_{\mathrm{system}}^{\mathrm{total}} \frac{\mathrm{PEC}_k^*}{\mathrm{PEC}_{\mathrm{total}}} \tag{49}$$

By using the equations presented above, $\dot{Z}_k^{\mathrm{total}}$ can also be written as

$$\dot{Z}_k^{\mathrm{total}} = 6.32 \cdot \mathrm{PEC_k} \cdot \frac{\phi}{\tau} \cdot \mathrm{CRF} \cdot (1 - \mu \cdot \mathrm{PWF}) \tag{50}$$

for a new system; replacing the factor of 6.32 with 4.16 for an extension of an existing system [33]. In the following, the superscript 'total' will be removed from the symbol $\dot{Z}_k^{\mathrm{total}}$.

The following values have been used in the calculation of the levelised capital investment cost rates: i = 10 %, μ = 12 %, ϕ = 1.06 and n = 20. The annual hours of operation τ have been varied between 100 and 8000. The purchased equipment costs have been determined by use of Aspen Plus V10 for the components of the organic Rankine cycle and the electrolysis water preheater. The equation of Oi and Wang for the cost of PEM electrolysis as function of hydrogen production in standard cubic meters per hour [24] is employed. The following equation for the PEC of a generator as function of its power output in kilowatt [34]

$$\mathrm{PEC}_{\mathrm{generator}} = \$60 \cdot \dot{W}_{\mathrm{generator}}^{0.95} \tag{51}$$

2.9.2 Cost rate balance equations

The cost rates for energy transport by mass, heat and work are $\dot{C}_{\text{mass}} = \dot{m}c\psi$, $\dot{C}_{\text{heat}} = c_{\dot{Q}}\dot{X}_{\dot{Q}}$ and $\dot{C}_{\text{work}} = c_{\dot{W}}\dot{X}_{\dot{W}}$ [32] where c, $c_{\dot{Q}}$, and $c_{\dot{W}}$ are the specific exergy costs of a mass flow, heat and power respectively. They are used in the cost rate balance together with the cost rate of a given component k, $\dot{Z}_k$, for the process happening in component k

$$\sum_{\text{input } i} \dot{C}_i + \dot{Z}_k = \sum_{\text{ouput } j} \dot{C}_j \tag{52}$$

Table 1 shows the cost rate balances for each component in concept together with the necessary auxiliary equations. The auxiliary equations are set up according to the F- and P-principles (fuel and product) explained in references [32] and [33]. For simplicity, the heat exchanging processes, that transfer thermal energy to and from the ORC working fluid, are simplified. Only one heat exchanger is used in both cases instead of five (steam to ORC working fluid (evaporator)) and two (ORC working fluid (condenser) to cooling water). For compression and liquefaction, the exergy rate of the heat loss/removal has been set to zero with $\dot{X}_{\dot{Q}_{\text{compr,out}}} = 0$ and $\dot{X}_{\dot{Q}_{\text{liq.,out}}} = 0$, respectively as the thermal energy removed from the hydrogen is rejected to the surroundings.

Table 1. Cost rate balances and auxiliary equations for the all components. The letters F and P denote on which of either F- or P-principle an auxiliary equation is based.

component	**cost rate balance**	**auxiliary equation(s)**
ORC evaporator	$\dot{C}_6 - \dot{C}_{9a} + \dot{Z}_{HX1} = \dot{C}_1 - \dot{C}_4$	$c_{9a} = c_6$ (F)
ORC turbine	$\dot{C}_1 + \dot{Z}_{\text{turbine}} = \dot{C}_2 + \dot{C}_{\dot{W},\text{turbine}}$	$c_2 = c_1$ (F)
ORC condenser	$\dot{C}_2 - \dot{C}_3 + \dot{Z}_{HX2} = \dot{C}_{13a} - \dot{C}_{11}$	$c_3 = c_2$ (F)
ORC pump	$\dot{C}_3 + \dot{C}_{\dot{W},\text{pump}} + \dot{Z}_{\text{pump}} = \dot{C}_4$	-
generator	$\dot{C}_{\dot{W},\text{turbine}} + \dot{Z}_{\text{generator}} = \dot{C}_{\text{electricity}}$	-
preheater	$\dot{C}_{15} + \dot{C}_{\dot{Q}_{\text{preheat}}} + \dot{Z}_{\text{preheater}} = \dot{C}_{16}$	-
electrolyser	$\dot{C}_{16} + \dot{C}_{\dot{W},\text{electrolysis}} + \dot{Z}_{\text{electrolyser}} = \dot{C}_{H_2} + \dot{C}_{O_2} + \dot{C}_{\dot{Q}_{\text{process}}}$	$c_{O_2} = c_{H_2}$ (P); $c_{\dot{Q}_{\text{process}}} = c_{\dot{W},\text{electrolysis}}$ (P)
compression	$\dot{C}_{H_2} + \dot{C}_{\dot{W},\text{compressor}} + \dot{Z}_{\text{compressor}} = \dot{C}_{H_2,\text{compr.}} + \dot{C}_{\dot{Q}_{\text{compr.,out}}}$	$c_{\dot{Q}_{\text{compr., out}}} = c_{\dot{W},\text{compressor}}$ (P)
liquefaction	$\dot{C}_{H_2} + \dot{C}_{\dot{W},\text{liquefaction}} + \dot{Z}_{\text{liquefaction}} = \dot{C}_{H_2,\text{liq.}} + \dot{C}_{\dot{Q}_{\text{liq.,out}}}$	$c_{\dot{Q}_{\text{liq., out}}} = c_{\dot{W},\text{compressor}}$ (P)

There are several known initial values for exergetic unit cost, which help solve the cost rate balances. The exergetic unit cost of steam in state 6 is equal to the unit cost of steam ($c_6 = c_{\text{steam}}$) as determined in Section 2.9.3. The cost of cooling water (state 11) and water supply to the electrolyser (state 15) is

assumed to be negligible ($c_{11} = 0$ and $c_{15} = 0$). Preheating is assumed to be carried out with available process heat (steam). Therefore, the necessary heat has the same exergetic unit cost as steam ($c_{\dot{Q}_{\text{process}}} = c_{\text{steam}}$). The heat removed or lost from the hydrogen compressor or liquefaction process is assumed to be transferred to the surroundings. Their exergy rates are considered to be zero ($\dot{X}_{\dot{Q}_{\text{compr.,out}}} = 0$ and $\dot{X}_{\dot{Q}_{\text{liq.,out}}} = 0$). ORC-pump, electrolyser, hydrogen compressor and hydrogen liquefactor are supplied with electricity produced either by the generator or with auxiliary electricity (except the ORC pump, which is not in operation, when auxiliary electricity is used). The exergetic unit cost is in these cases equal to the exergetic unit cost of electricity ($c_{\dot{W},\text{pump}} = c_{\text{electricity}}$, $c_{\dot{W},\text{electrolysis}} = c_{\text{electricity}}$, $c_{\dot{W},\text{compressor}} = c_{\text{electricity}}$, $c_{\dot{W},\text{liquefaction}} = c_{\text{electricity}}$).

From the above there are eight unknowns in the eight cost rate balances, which are c_1, $c_{\dot{W},\text{turbine}}$, c_{13a}, c_4, $c_{\text{electricity}}$, c_{16}, c_{H_2} and $c_{\text{H}_2,\text{compr.}}$ or $c_{\text{H}_2,\text{liq.}}$. The set of equations can be solved by using the equations to solve for c_4 first, and then solving for the other cost coefficients in the order c_1, $c_{\dot{W},\text{turbine}}$, c_{13a}, $c_{\text{electricity}}$, c_{16}, c_{H_2} and $c_{\text{H}_2,\text{compr.}}$ or $c_{\text{H}_2,\text{liq.}}$.

2.9.3 Cost of steam

In order to solve the thermo-economic equations, the cost of steam (c_{steam} or c_6 in the context of the presented ORC-concepts and cost balances in Table 3) entering the heat exchanger to the ORC-working fluid has to be known. The cost of steam (in $/kg) can in general be calculated by

$$c_{\text{steam}} = c_{\text{energy}}(h_{\text{steam}} - h_{\text{feedwater}}) \tag{53}$$

where c_{energy} is the energy unit cost (in $/kJ) and h_{steam} and $h_{\text{feedwater}}$ are the specific enthalpies of the steam leaving the boiler and the feedwater entering the boiler in kJ/kg. In the specific case of municipal solid waste incineration, this material is the energy source for the steam generation in the boiler, the unit cost of energy can be calculated by

$$c_{\text{energy}} = \frac{c_{\text{waste collection}}}{\text{LHV}_{\text{waste, as received}}} \tag{54}$$

In this equation, $c_{\text{waste collection}}$ is the cost of waste collection per tonne of municipal solid waste and $\text{LHV}_{\text{waste, as received}}$ is the lower heating value of the waste, as it is received and fed into the incinerator. The cost of waste collection and transportation to the Bergen CHP plant in 2018 was given as NOK 1000 per tonne by the local waste management operator BIR AS [35]. A currency conversion factor of 7.8 NOK/$ was applied [36]. The lower heating value of the as received waste incinerated in the local municipal solid waste incineration plant has been estimated to be 13.557 MJ/kg in the year 2013 in earlier studies [4, 37]. The resulting cost per energy unit is $9.46/GJ. The thermodynamic states of feedwater and steam are $T_{\text{feedwater}}$ = 131.2 °C, $P_{\text{feedwater}}$ = 65 bar(abs) and T_{steam} = 402 °C, P_{steam} = 42.5 bar(abs) respectively [5]. The corresponding specific enthalpies are $h_{\text{feedwater}}$ = 555.74 kJ/kg and h_{steam} = 3216.1 kJ/kg. The result is a unit cost of steam equal to $0.0251/kg.

2.9.4 Cost of PEM electrolysis

The purchased equipment cost for the electrolyser has been estimated with the equation of Oi et al. [24] given in € in ref. [38]. To convert to 2018 US$, the currency was first converted with the average 2010 exchange rate of $1.327/€ [39] and then adjusted for inflation with an average inflation rate of 2.5% for US$ [40]. Converted to 2018 US$ the equation reads

$$\mathrm{PEC}_{\mathrm{electrolysis}} = \$40208 \frac{\dot{V}_{\mathrm{H}_2}^{0.79}}{J^{0.32}} \tag{55}$$

where $\dot{V}_{H_2}$ must be given in standard cubic meter per hour. The lifetime of an electrolyser cell of 60 000 h was assumed so that at least three sets of electrolysers have to be obtained during the 20 year lifetime of the facility.

2.9.5 Cost of H_2 compression

At a volume flow rate of 300 standard cubic meters per hour of hydrogen (known capacity), the purchased equipment cost (PEC) of a hydrogen compressor is \$320 000 (PDC diaphragm compressor [41]). The cost for other volume flows is based on the power law [33]

$$\mathrm{PEC}_{\mathrm{compression}} = \$320\,000 \left(\frac{\dot{V}_{H_2}}{300\ \mathrm{m}^3_{\mathrm{standard}}/\mathrm{h}} \right)^{0.6} \tag{56}$$

where the hydrogen volume flow $\dot{V}_{H_2}$ must be given in $\mathrm{m}^3_{\mathrm{standard}}/\mathrm{h}$.

2.9.6 Cost of H_2 liquefaction

The purchased equipment cost of H_2 liquefaction is based on data for the total installed cost published by Elgowainy et al. [42]. According to Bejan et al. the purchased equipment cost can be calculated from the total installed cost by dividing by 1.45 if no further information about installation costs is available [33].

$$\mathrm{PEC}_{\mathrm{liquefaction}} = \$36\,624\,824 \left(\frac{\dot{m}_{\mathrm{H}_2}}{19.56\ \mathrm{tonne/d}} \right)^{0.6471} \tag{57}$$

2.10 Work flow and optimisation

The objective of the optimisation process was to find the maximum net power output of the ORC turbine (equation (12)). The built in problem solver in Microsoft Excel® with its GRG-non-linear solver was employed for this task. The properties whose values need to be specified in advance are given in Table 2. It gives an overview of the input data necessary to populate the equations of the model, which has been realised in Microsoft Excel® with the CoolProp addin [28].

The work flow was as follows. Initial values for temperature T_1, maximum and minimum pressure (P_{min} and P_{max}) of the ORC-working fluid and the pressure of the condensing steam (P_{source}) were entered in order to obtain process paths and an ORC-curve as shown in Figure 4. The properties varied by the solver in the different concepts in order to maximise the ORC net power output were the temperature at the turbine inlet (T_1), and the minimum pressure (P_{min}) and maximum pressure (P_{max}) of the ORC working fluid. In concept B, the value of z_{el} (see equation (33)) needed to be given in advance as well. It was then varied by the solver such that the sum of the electrolysis power and the corresponding actual compression/liquefaction power were equal to the available electric power from the ORC.

The relevant constraints for the optimisation were as now follows.

A minimum pinch point temperature difference between heat source and ORC-working fluid is assured by the constraint $\Delta T_{\mathrm{pp,source}} \geq \Delta T_{\mathrm{pp,source,min}}$. $\Delta T_{\mathrm{pp,source}}$ is the minimum of the six temperature differences $T_6 - T_1$, $T_{7'} - T_{1''}$, $T_7 - T_{1'}$, $T_8 - T_5$, $T_{8'} - T_{4'}$ and $T_{9a} - T_4$. Minimum pinch point temperature differences of 5°C were used as in previous work [17, 43].

In order to keep the organic Rankine cycle subcritical the constraint $P_{\mathrm{max}} \leq P_{\mathrm{cr,\,ORC}} - 250\ \mathrm{kPa}$ was used. This also kept the cycle in a region of the phase diagram where the thermodynamic properties of the working fluid are known. This constraint is necessary for CoolProp to work properly.

A large enough temperature is needed in the ORC-working fluid to be able to remove the waste heat from the organic Rankine cycle to a heat sink with reasonable mass flow rate. This is assured by the constraint $P_{\mathrm{min}} \geq P_{\mathrm{sat}}(T_0 + \Delta T_{\mathrm{condens.}})$.

A high enough quality at the end of the ORC-working fluid expansion process in the turbine is assured by the constraint $x_2 \geq 90\%$.

A number of other constraints had to be defined whose sole purpose was to obtain thermodynamically correct behaviour of all involved state variables while the solver was trying different solutions.

The thermo-economic analysis was carried out based on output from the ORC-worksheet.

Table 2. Input data to the work sheet where the ORC-calculations and optimisation is carried out.

Fluid/process	**Property**	**Comment**
ORC-working fluid	$P_{\mathrm{max}}, P_{\mathrm{min}}$	Maximum and minimum pressure in the cycle; later varied by the solver within given constraints. P_{max} is the pressure between pump outlet and turbine inlet, P_{min} is the pressure between turbine outlet and pump inlet.
	$T_{\mathrm{max,ORC}} = T_1$	Temperature at turbine inlet (max. temperature of ORC-fluid); later varied by the solver within the constraint given by the minimum allowed temperature difference to the steam.
	$\eta_{s,\mathrm{pump}}, \eta_{s,\mathrm{turbine}}$	Isentropic efficiencies of pump and turbine; set to 0.85 and 0.9 respectively.
	$\varepsilon_{\mathrm{evap}}, \varepsilon_{\mathrm{cond}}, \varepsilon_{\mathrm{preheat}}$	Effectiveness of heat exchangers: ORC evaporator, ORC condenser and electrolysis water preheater; all are set to 0.8.
	$\Delta T_{\mathrm{superheat,min.}}$	Minimum superheating over saturation temperature at P_{max}; used to guarantee dry vapour at turbine inlet. It must be positive and is set to 0.05°C.

	$\Delta T_{\mathrm{pp,source,min}}$	Minimum temperature difference between working fluid and heat source fluid during heating and evaporation; set to 5°C; used as constraint.
	$\Delta T_{\mathrm{pp,sink,min}}$	Minimum temperature difference between working fluid and heat sink fluid during condensation; set to 5°C; used as constraint.
Waste heat fluid	T_6 or x_6	Maximum temperature of the heat source fluid (if superheated) or its quality (if a saturated mixture comes from the steam turbine) has to be set.
	$\Delta T_{\mathrm{subcool}}$ or x_{9a}	Either the degree of subcooling below the saturation pressure of the condensing steam or the quality of the liquid-vapour-mixture at the outlet of preheater 1 has to be given in order to define state 9a.
	P_{source}	Pressure in all states of the heat source fluid.
	$\dot{m}_{\mathrm{source}}$	Mass flow of the heat source fluid.
Heat sink fluid	$T_{\mathrm{min,\ sink}} = T_{11}$	Minimum temperature in heat sink fluid; initially set to T_0.
	$P_{\mathrm{sink}} = P_{11}$	Pressure used in all states of the heat sink fluid.
	$\Delta T_{\mathrm{heat\ sink,max}}$	Maximum allowed temperature rise in heat sink fluid. It is set to 20 °C, which in the context of this work limits the outlet temperature to 30°C.
Surroundings	T_0, P_0	Temperature and pressure of the surroundings.
Electrolysis	η_{gen}	Generator efficiency.
	J_{target}	Current density in kA/m^2.
	$T_{\mathrm{electrolysis}}$	Electrolysis temperature.
Preheating	$\Delta T_{\mathrm{pp,preheat,min}}$	Minimum pinch point temperature between condensing steam and liquid water during preheating; set to 5°C; used as constraint.
Compression	η_{T}	Isothermal efficiency of the hydrogen compressor.
Liquefaction	$\eta_{\mathrm{II,liq.}}$	Second law efficiency of liquefaction process; calculated as function of hydrogen mass flow $\dot{m}_{\mathrm{H_2}}$.

3 Results

The mass flow rate of condensing steam ($\dot{m}_{\mathrm{source}}$) was set to 10 kg/s to align to an order of magnitude with the steam cycle of the CHP facility; whereby the calculations were motivated by ref. [4].

In the first round of calculations, optimal states for the ORC between the condensing steam and the ORC-cooling water were obtained by employing the solver add-in in Microsoft Excel. The ORC states were optimised for maximum net power output from the ORC. Figure 5 shows the ORC power output as function of steam condensing pressure in the interval from 80 to 200 kPa. For the sake of clarity, only the two best performing and the worst performing working fluids are shown. The largest output power is achievable with ethanol as working fluid, followed by R1233zd(E). The available power increases from 2.14 MW to 2.73 MW over the shown interval. The output from an ORC with R1233zd(E) as working fluid is between 6.8% - 11.7% lower compared with the ethanol-ORC. R1234yf, with its much lower critical temperature compared with the other fluids and also a more narrow saturation dome, has much lower power output (1.60 – 1.79 MW) and a slower increase over the interval between 80 and 200 kPa.

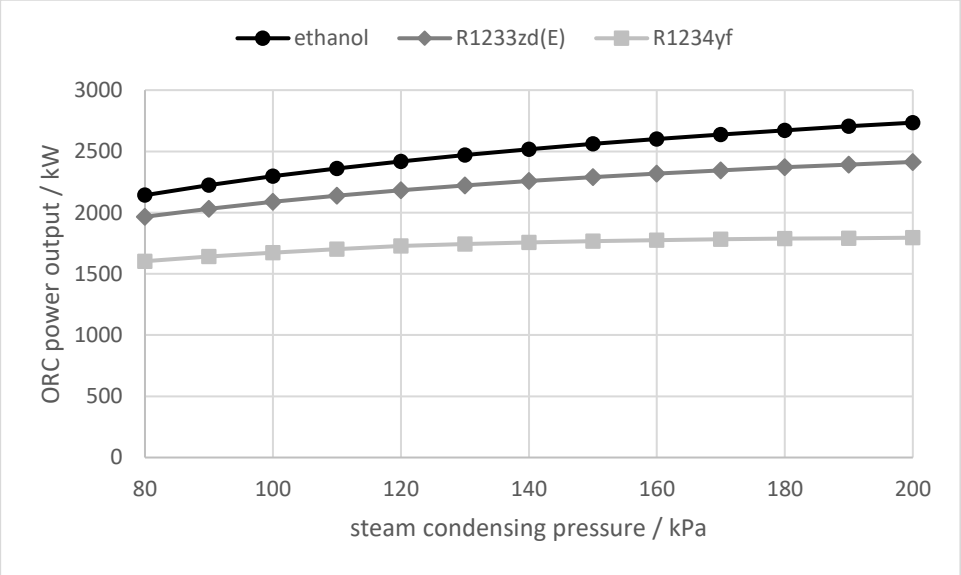

Figure 5. ORC output power as function of steam condenser pressure. The results for the two best performing working fluids and for the worst performing working fluid are shown.

Both ethanol and R1233zd(E) were taken into the further analysis of hydrogen production potential and production cost. Although an ASHRAE classification of ethanol does not exist, it is known to be flammable and toxic in pure form. Therefore, it might be unattractive as a working fluid in an actual facility. R1233zd(E) with its A1 classification belongs to the group of working fluids with the lowest classification with regard to both toxicity (A) and flammability/flame spreading (1) and could therefore be the preferred choice, even if the power output from the ORC is lower than ethanol.

The hydrogen production potential in g hydrogen per kg condensed steam is shown in Figure 6 for both working fluids ethanol and R1233zd(E) and both concepts A and B. Values range from 0.991-1.27 g H_2/kg steam (ethanol) and 0.872-1.12 g H_2/kg steam (R1233zd(E)) within the investigated pressure interval respectively for concept A. When all ORC output power is used for both electrolysis

and post-processing (compression or liquefaction within concept B), the maximum production rate is between 0.950 to 1.21 g H_2/kg steam for ethanol (compressed H_2). The lowest rates are for liquid hydrogen produced with R1233zd(E) as a working fluid with 0.647-0.794 g H_2/kg steam. The increase and shape of the curves follows those of the ORC output power in Figure 5. The use of concept B and compression of hydrogen to 350 bar consumes 4.2% of the produced electric power, while liquefaction requires 28.9%, respectively.

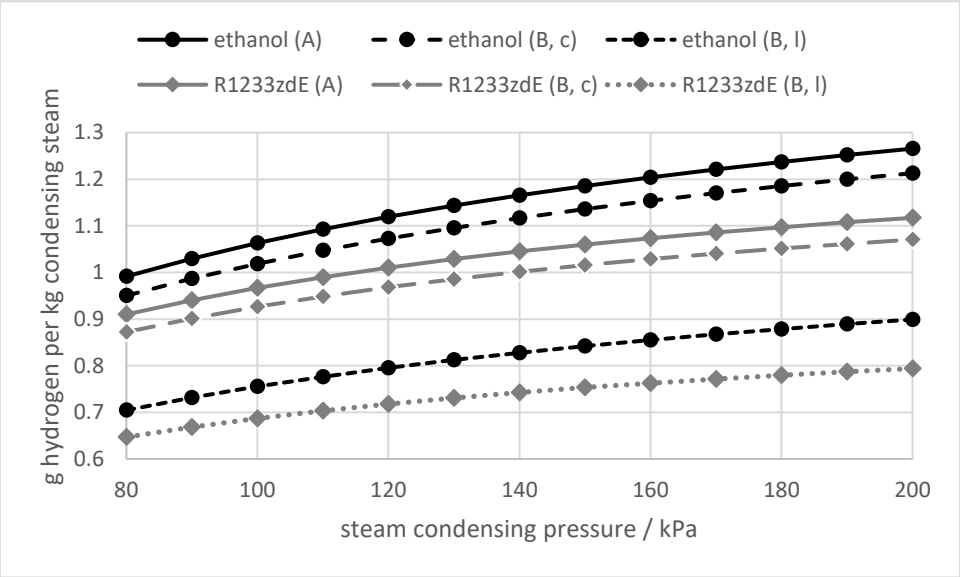

Figure 6. Hydrogen production potential for the two different working fluids within the different production concepts (A and B) as function of steam condensing pressure.

Based on a steam mass flow of 10 kg/s, the production capacity ranges from 259 m^3 H_2/h in the worst case (R1233zd(E), 80 kPa steam condensing pressure, concept B with liquefaction) to 507 m^3 H_2/h in the best case (ethanol, 200 kPa steam condensing pressure, concept A). The annual production at 8000 hours operation time will therefore lie between 186 tonne H_2 in the worst case and 364 tonne H_2 in the best case.

The energy efficiency (or first-law-efficiency) of the hydrogen production concepts is mainly connected to the efficiency of the electrolysis model [23]. Values are 68.2% for uncompressed gaseous hydrogen directly from the electrolyser, 65.4% for compressed hydrogen (350 bar) and 48.6% for liquid hydrogen for both concept A and B and both working fluids.

The second law efficiency of concept A (equation (36)) is also independent of the ORC working fluid with values of 5.41% directly from the electrolyser, 8.33% for compressed hydrogen (350 bar) and 7.60% for liquid hydrogen. When concept B is applied, the second law efficiencies (equation (38)) depend on the use of either compression or liquefaction as post-production method. Equations (36) and (38) are based on the work potential of the generated electric power by the organic Rankine cycle and other energy inputs to hydrogen production. Concept B and compression has a second law efficiency of 5.18% and 8.31% for uncompressed and compressed hydrogen respectively. In case of liquefaction, the values are 3.85% and 7.49% for gaseous and liquid hydrogen.

When the expended exergy contribution of the work input from the organic Rankine cycle is replaced by the exergy rate change of the condensing steam (equations (37) and (39)), the second law efficiency changes with condenser pressure as shown in Figure 7 for concept A. The reason for the second law efficiency of the liquefied hydrogen being largest is the contribution of the thermal exergy of the hydrogen, which recovers a part of the work input to the liquefaction process.

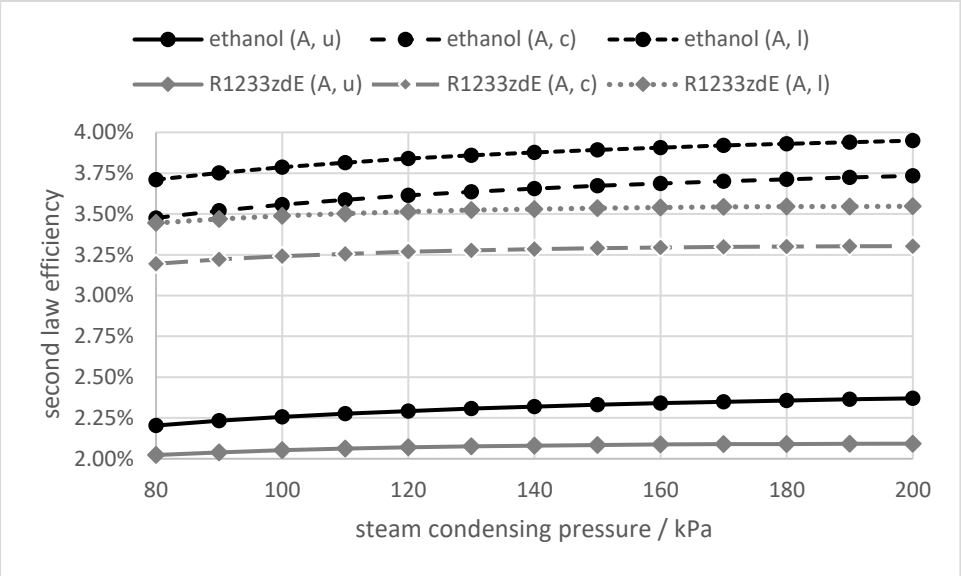

Figure 7. Second-law-efficiency of the hydrogen production process in concept A for uncompressed (u), compressed (c) and liquefied (l) hydrogen according to equations (37) and (39).

The second law efficiency values lie in the same range for concept B (Figure 8), however being slightly smaller for the gaseous hydrogen directly from the electrolyser, as no auxiliary power is used for compression and liquefaction. This also leads to the values for compressed hydrogen being slightly lower compared to concept A (only 4.2% of the generated electricity is used for compression). Even though 28.9% of the generated electricity is used for liquefaction in concept B, the second-law-efficiency is lower than that of compressed hydrogen production, because less hydrogen is produced, that could recover the steam's exergy.

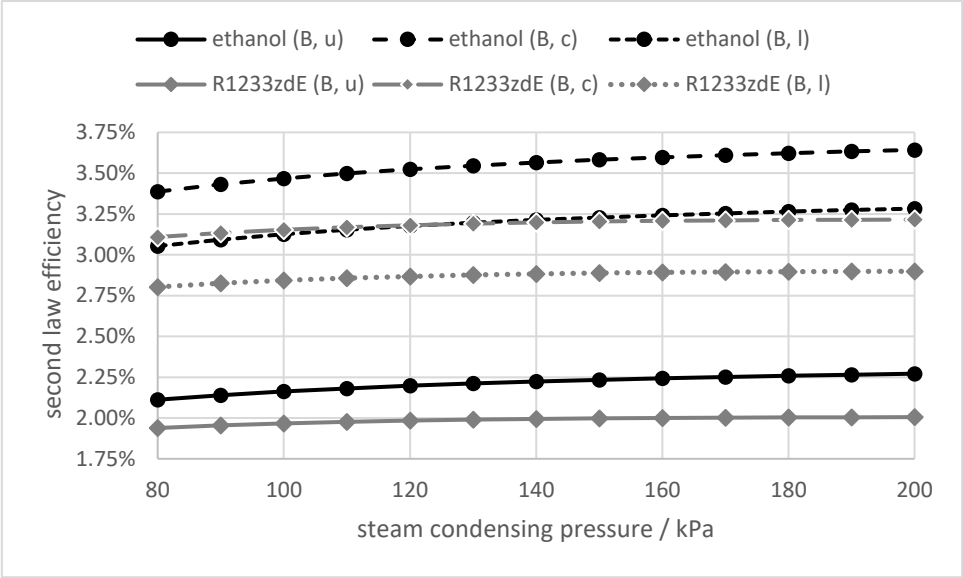

Figure 8. Second-law-efficiency of the hydrogen production process in concept B for uncompressed (u), compressed (c) and liquefied (l) hydrogen according to equations (37) and (39).

Figure 9 shows the average cost of hydrogen production as function of hours of waste heat use for ethanol as ORC working fluid and a steam condensing pressure of 80 kPa. A cost of steam of $0.0251/kg (see Section 2.9.3) is taken into account. The hydrogen production cost is on average 1.2% higher at minimum waste heat use compared with maximum waste heat use. As can be expected, the uncompressed hydrogen directly from the electrolyser has the lowest production cost, as the following post-processing equipment does not affect its cost. The cost decreases from $9.91 at 250 hours of waste heat use to $9.75 at 8000 hours (the full operational time per year). The production cost is almost identical for compressed hydrogen (350 bar) in concepts A and B, as only 4.2% of the electricity produced by the ORC is needed to compress the hydrogen. The difference in production cost for liquid hydrogen is more distinct: $24.99 from concept A and $27.45 from concept B at 250 hours of waste heat use, and $24.83 and $27.23 when waste heat is available for the full operational time of 8000 hours.

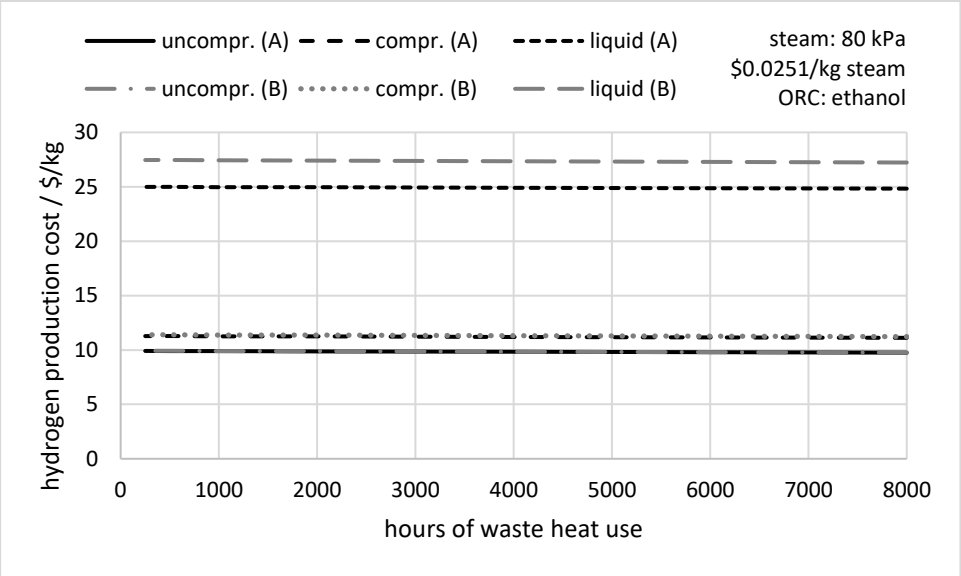

Figure 9. Average hydrogen production cost as function of hours of waste heat use.

In comparison, Figure 10 shows the average hydrogen production cost as function of hours of waste heat use when the steam is supplied at no cost to the heat exchanger with the ORC. This corresponds to a situation where it is regarded as pure waste heat that can serve no other purpose and would otherwise be rejected to the surroundings. Compared with Figure 9, the costs decrease in a much more pronounced manner with an increasing use of waste heat.

Compared to the curves in Figure 9 (with steam cost), the difference in hydrogen production cost at low waste heat use in Figure 10 (no steam cost) is on the average 2.2% lower. The small difference is due to steam playing a minor role in this context. The ORC is hardly used and in both concepts: mainly auxiliary electric power is used in hydrogen production. Therefore, the hydrogen production cost decreases more severely with an increasing number of hours of waste heat use when the cost of steam is zero (Figure 10) compared with a non-zero cost of steam (Figure 9). By way of example, the hydrogen production cost is 27.3%-66.5% lower when the steam is considered to have no cost at 8000 hours of waste heat use. The differences are smaller for liquid hydrogen compared to gaseous hydrogen, which has the largest difference.

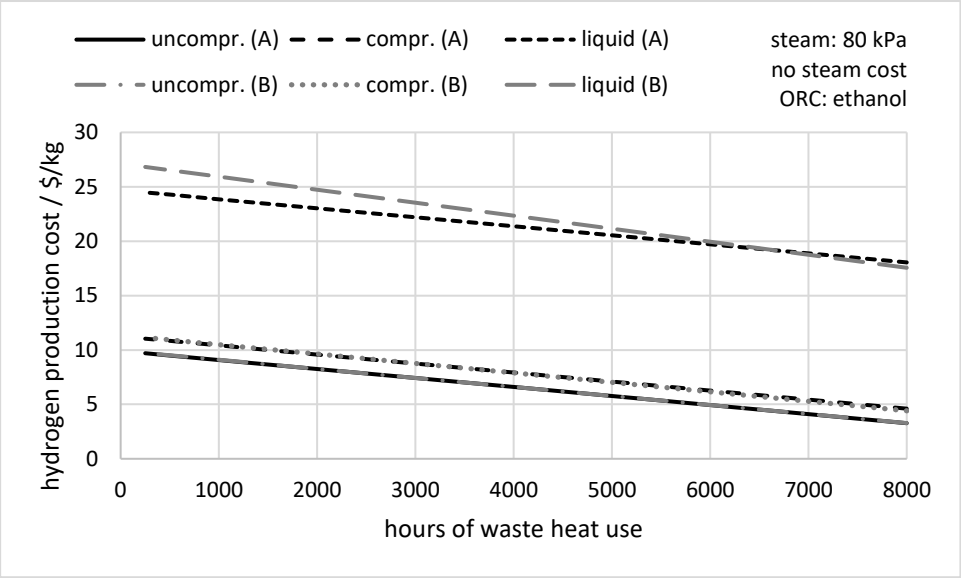

Figure 10. Average hydrogen production cost as function of hours of waste heat use.

The cost of compressed hydrogen at a given number of hours of waste heat use is almost identical in concepts A and B while there is a clear difference for liquid hydrogen. Concept B as the slightly larger production cost for compressed hydrogen and the cost is lower from about 750 hours; however, the difference in production cost is insignificant between the two concepts. The decrease in production cost of liquid hydrogen with increasing hours of waste heat use is slightly stronger for concept B than for concept A with a higher cost at low waste heat use. That said, the lines representing the production cost cross at around 7000 hours of waste heat use, such that concept B does not give a clear advantage in production costs even when waste heat is available for the full annual operating time. It might be wise to compare the cost of electricity produced by means of the ORC as function of hours of waste heat use with the price for auxiliary electricity in order to find the minimum number of hours that waste heat needs to be available for either concept to be cost competitive.

Although the production rate differs with changing steam condensing pressure, the associated difference in hydrogen production cost is negligible. It is \$0.03/kg H_2 at no steam cost for the uncompressed hydrogen directly out of the electrolyser and a maximum of \$0.14 \$0.03/kg H_2 with steam cost. For compressed hydrogen (350 bar) the cost is ca. \$0.06/kg H_2 lower at 200 kPa steam condensing pressure (see Figure 11). For liquid hydrogen, the difference is larger, ca. \$1.0/kg H_2 between 80 kPa and 200 kPa steam condensing pressure both with and without steam cost. The production cost is smaller at the higher condensing pressure.

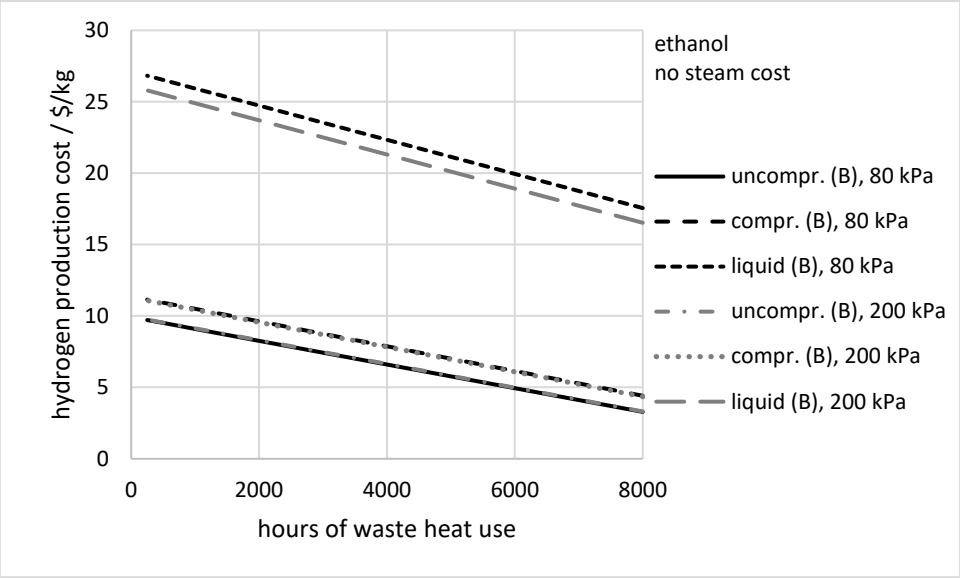

Figure 11. Comparison of hydrogen production cost at different steam condensing pressure as function of the number of hours of waste heat use.

A comparison between the two working fluids shows that differences in in hydrogen production costs are small (typically less than \$0.3/kg H_2), with R1233zd(E) having the lower production cost of the two working fluids. This is the case not only for the situation shown with 80 kPa steam condensing pressure and no steam cost, but a general feature of the results at a given steam condensing pressure and the same steam cost. The purchased equipment cost (PEC) and therefore the total capital investment (TCI) are on the average 10% lower when using R1233zd(E) as working fluid. The lower production rate results in smaller equipment size, which is cheaper. However, as the use of ethanol as ORC-working fluid yields between 8.9% (80 kPa) to 13.3% (200 kPa) higher hydrogen output, the focus will be on results obtained with ethanol as ORC-working fluid in the following.

Figure 12 shows the cost of electricity produced by the ORC as function of hours of waste heat use for 80 kPa as steam condensing pressure. At 200 kPa, the cost is only negligibly higher for both working fluids at the large end of the scale, while the ORC-generated electricity cost is larger at 250 hours waste heat use at 200 kPa steam condensing pressure compared to 80 kPa. The cost per kWh electricity is an inverse function of the number of hours. The cost of electricity generated by the energy recovered will only be cheaper than the auxiliary electricity when the cost of steam is neglected and at least ca. 2000 hours of waste heat use. Both numbers are smaller than the average time that waste heat is available (ca. 3000 hours) in the CHP facility in Bergen. At full time use of waste heat (8000 hours) and no steam cost, the cost of electricity generation is just \$0.0329/kWh (R1233zd(E)) and \$0.0349/kWh (ethanol) respectively.

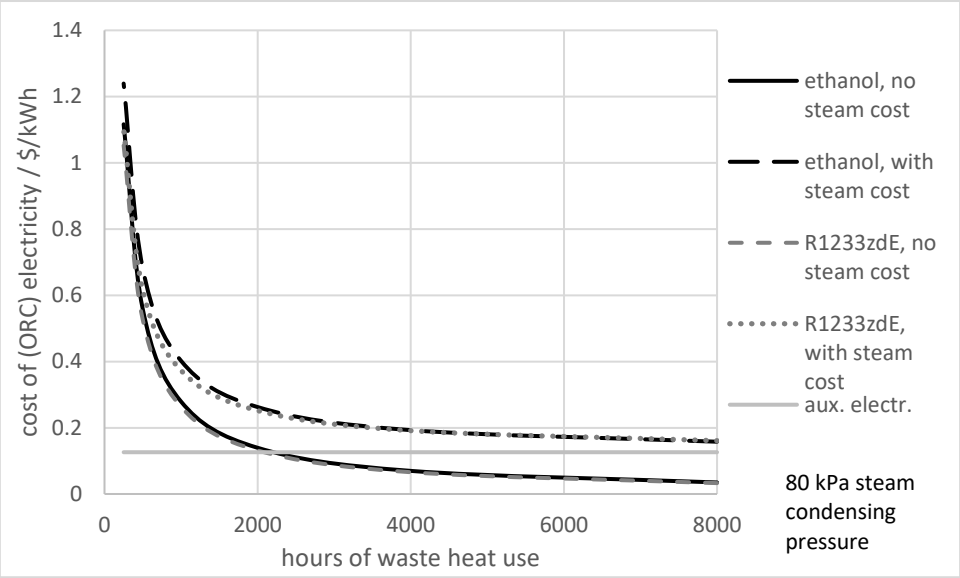

Figure 12. Comparison of the cost of electricity generated with energy recovered by the ORC and the cost of auxiliary electricity.

The purchased equipment cost for the electrolysis equipment is 2.27-times larger at 1 kA/m^2 than at 10 kA/m^2. However, larger current density means also a less efficient electrolysis and therefore a lower hydrogen production rate. The difference in production potential lies between 20-35 tonne per year more hydrogen depending on production concept (A or B) and final state of the hydrogen, which corresponds to 11% greater production potential at 1 kA/m^2 rather than at 10 kA/m^2.

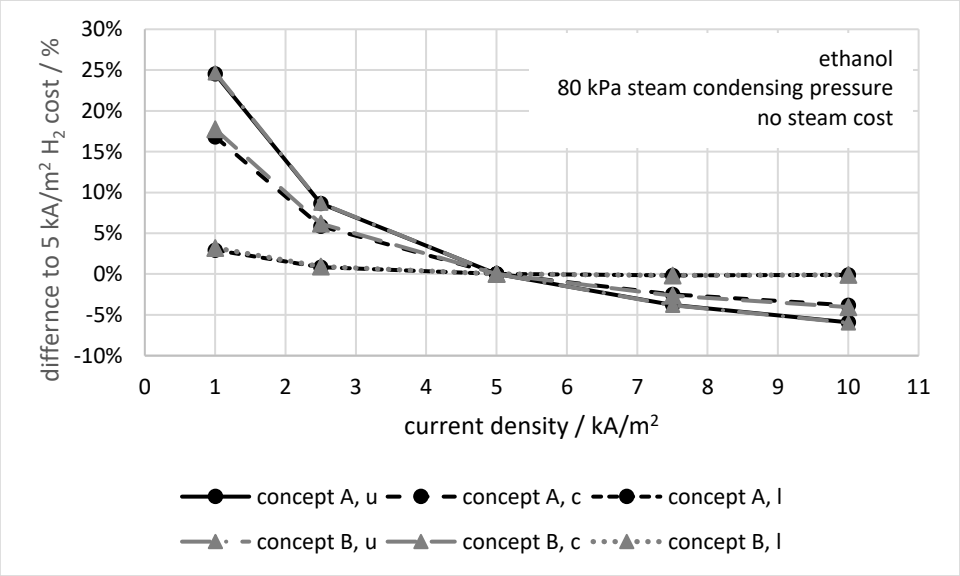

Figure 13. Variation of hydrogen production cost with ethanol as ORC working fluid for uncompressed (u), compressed (c) and liquefied hydrogen (l) when the cost of steam is neglected.

Figure 13 shows the variation of the hydrogen production cost as function of the current density relative to the cost at 5 kA/m^2 current density for ethanol as ORC working fluid and 80 kPa steam condensing pressure. It is a typical example for the other combinations of working fluid and condensing pressure without steam cost taken into account. The cost varies less than 1% for liquefied hydrogen from both production concepts A and B between 2.5 and 10 kA/m^2. While the curves fall monotonic

for uncompressed and compressed hydrogen from both concept A and B. When the cost of steam is taken into account (see Figure 14), the deviation from the 5 kA/m^2 cost is generally smaller. The maximum deviation occurs for concept A at 250 hours of waste heat use and 4% larger, followed by 3.3% for compressed hydrogen from both concepts. The curves now show minima along the current density axis. It lies around 5 kA/m^2 for uncompressed and compressed hydrogen and around 2.5 kA/m^2 for liquid hydrogen.

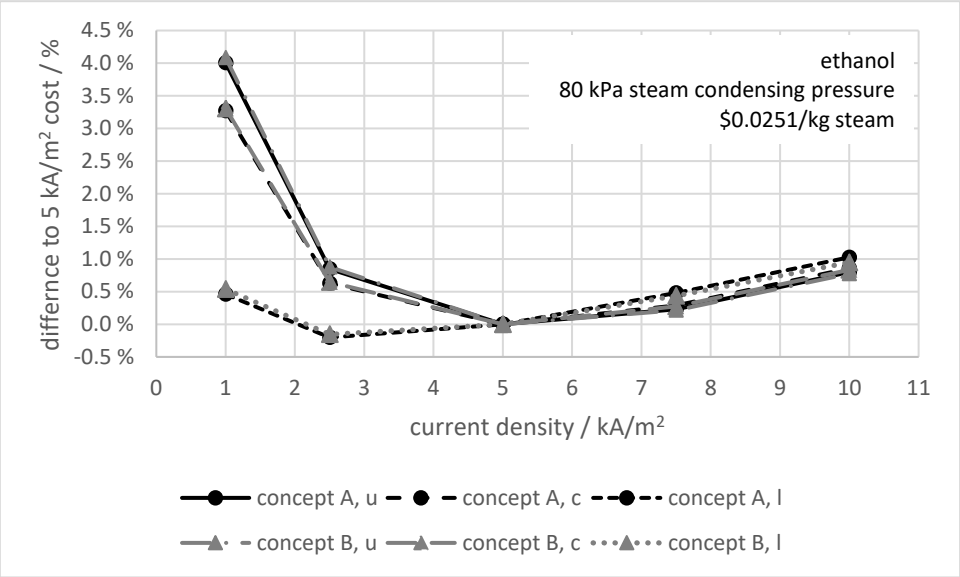

Figure 14. Variation of hydrogen production cost with ethanol as ORC working fluid for uncompressed (u), compressed (c) and liquefied hydrogen (l) when the cost of steam is taken into account.

The final question to be answered is: who could be a customer for the produced hydrogen? As transport and storage of hydrogen is still an expensive task, it would be advantageous to have immediate use by either fuelling vehicles at or near the site of production or by a co-located chemical process plant. Presently, the waste management operator BIR AS, Bergen, Norway, which has been the focus for this study, has a fleet of 49 waste collection vehicles plus 5 vehicles in reserve [44]. A typical waste collection vehicle operating on compressed hydrogen stored at 350 bar uses about 5.5 kg hydrogen per day [27]. An amount of 70.1 tonne compressed hydrogen is needed to run the full fleet of waste collection vehicles on 260 days per year (weekends excluded) for waste collection. The smallest amount of hydrogen that can be produced per year with concept B is 251 tonne with R1233zd(E) as ORC working fluid receiving thermal energy from condensing steam at 80 kPa (which is also the scenario with the lowest total capital investment: $11.2 million). As such, three times this number of vehicles could be operated. This opens for the possibility to let other customers buy the excess hydrogen. A potential customer could be the local public transport operator, who has a depot with a capacity of 86 busses nearby. If busses from this fleet ran on hydrogen, each of them would have an average annual consumption of 3.83 tonne hydrogen [25], based on their annual driving distance and consumption. The remaining hydrogen would be enough to supply 47 hydrogen-powered busses; if the busses used all produced hydrogen exclusively, 65 busses could be supplied year round. In early summer 2018, compressed hydrogen at 700 bar was sold at a price of ca. $11.54/kg [45] in Norway. The waste incineration plant in Bergen has ca. 3000 hours of waste heat available in the form of condensing steam at 80 kPa with a mass flow of slightly above 10 kg/s. At this number of hours with

waste heat use, the production cost of compressed hydrogen is \$8.78/kg H_2 without steam cost and \$11.22/kg H_2 with steam cost taken into account. Both costs are below the prize of compressed hydrogen at local filling stations (June 2018).

4 Discussion

While the hydrogen production potential measured in g H_2/kilogram steam exceeds that of the hydrothermal route investigated by Yilmaz and co-workers [6, 9], the exergy efficiency of the concepts investigated is much lower with only a few percent compared with more than 20%. This can in part be explained by the low temperature of the heat source, which condenses steam at temperatures between 93.49°C (80 kPa) and 120.21°C (200 kPa). The Carnot-efficiencies available with a heat sink temperature of 10°C lie between 22.7% and 28%. About half of this thermal efficiency can be achieved with the ORC-unit. Another reason for the low second law-efficiencies is the large exergy rate change of the condensing steam, which appears in the denominator of the second law-efficiency, next to the other energy inputs to the process. At a mass flow rate of 10 kg/s, the change in exergy rate of the steam lies between 9.67 MW (80 kPa) and 11.1 MW (200 kPa). The ORC-fluid evaporator recovers less than half of this amount (for example 40% at 80 kPa and 41.5% at 200 kPa steam condensing pressure, respectively) in case of ethanol. The other energy inputs to the process are typically less than 200 kW, except for the liquefaction power, which can be about a megawatt. The exergy rate change of the condensing steam is therefore clearly the largest contribution to the exergy supplied to the process. The rate of recovered exergy is about 140 kW (uncompressed H_2) to 300 kW (liquid H_2) in concept A for ethanol. Set in relation with the exergy rate change of the steam as the major contribution to the expended exergy explains the low second law-efficiencies.

The energy efficiency of hydrogen production is largest for uncompressed hydrogen, and decreases for compressed hydrogen and is lowest for the liquefied hydrogen. This is due to the additional energy needed for compression and liquefaction, where the energy need for liquefaction is the largest. The sequence of second-law efficiencies is different between concept A and B due to the consideration of both the total exergy rate of the hydrogen in the final state of the process (lowest for uncompressed, largest for liquefied hydrogen) and the expended exergy. The mass flow of the produced hydrogen is independent of the energy need for compression or liquefaction in concept A because the full electricity output of the ORC-unit is used for electrolysis in concept A. The second law efficiency increases from uncompressed towards liquid hydrogen because the total specific exergy of the hydrogen increases from uncompressed to compressed to liquid hydrogen while the expended exergy is almost constant and dominated by the exergy change of the condensing steam.

The available electricity from the ORC unit must supply both the electrolyser and post-processing in concept B. The second law efficiency of the uncompressed hydrogen is still the smallest due to the lower exergy rate of the produced hydrogen. The energy and exergy demand for liquefaction are much higher compared with the compression and cannot be equally recovered in the final state of the hydrogen. The compression process demands less energy and exergy compared with the liquefaction process. It leaves more electricity for the electrolyser. The exergy rate of the recovered hydrogen is larger for compressed than for liquid hydrogen due to the larger mass flow of hydrogen in case of compression. The production of compressed hydrogen has therefore a larger second law efficiency than the production of liquid hydrogen in concept B.

Although a detailed analysis of exergy destruction rates in the different components has not been carried out, it is safe to assume, that the steam to ORC-working fluid heat exchanger, electrolyser and liquefaction process are the components with the lowest second law-efficiencies.

Despite the higher production potential (per kg steam), the calculated cost of a kilogram of uncompressed hydrogen is comparable to the cost given in ref. [6] ($3.14/kg H_2) only when the condensing steam has no cost. In the current work, the cost at 80 kPa is $3.27/kg H_2 with ethanol as ORC working fluid and $3.06/kg H_2 with R1233zd (E), respectively. It is also larger compared to $2.37/kg H_2 [9]. The exergetic unit cost of electricity produced by the ORC of $0.04/kWh obtained by Yilmaz et al. [6] is comparable with the results in this work when waste heat is used for at least 2/3^{rds} of the year at no steam cost. An overview of hydrogen production cost published by the U.S. Drive Partnership (a collaboration of the U.S. Department of energy and commercial partners) shows costs of $3.50/kg H_2 to $6.50/kg H_2 for high volume production (>50 tonne per day) by PEM electrolysis [46]. This price range could be achieved from about more than 4000-4500 hours of waste heat use for no steam cost in the studied concepts.

The model for calculation of the hydrogen yield from the PEM electrolyser uses properties of a Nafion membrane and is from 2008 [23]. Advances in PEM technology have been made since and more efficient and cheaper materials are available [40]. Further reductions in equipment cost can be expected, mainly due to scaling up of production [16]. For the studied concepts with compressed hydrogen as final product, the electrolysis equipment is about 27%-29% of the total equipment cost: 8.6%-9.6% for those with liquid hydrogen. Even though the cost of PEM electrolysis equipment is expected to drop by up to 25% [16] in the future, it will not be able to contribute to a large reduction of liquid hydrogen production costs in the investigated concepts, while the cost of compressed hydrogen would drop further.

The extrapolation of the second-law-efficiency of hydrogen liquefaction for the calculation of the necessary liquefaction power introduces some uncertainty into the results connected to liquefaction. In the absence of own experimental data and other published results on the second law-efficiency of liquefaction, the extrapolation was the best available tool to the authors.

The cost estimate is limited because there was not enough information available to do a full analysis following the procedure given in the book by Bejan et al [33]. Therefore, the total capital investment was based on the purchased equipment cost. The factor of 6.32 was taken to estimate TCI. In case the hydrogen production facility could be realised on available land, it could be treated as an extension of an existing plant and a factor of 4.16 would be used in the cost analysis. This would lead to a reduction in the cost per kilogram of hydrogen of about 6% on the average.

The total capital investment ranges from the aforementioned $11.2 million (concept B, 80 kPa steam condensing pressure, R1233zd(E) and compression to 350 bar, 251 tonne H_2/a, $11.22/kg-$11.46/kg with steam cost) to $45.1 million (concept A, 200 kPa steam condensing pressure, ethanol, liquefaction, 364 tonne H_2/a, $23.96/kg-$24.03/kg). The cost of liquid hydrogen production by the proposed concepts is larger than current market prices, while the cost of compressed hydrogen is comparable with current prices in Norway. The reason for the large cost for liquid hydrogen may be the low production capacity [42]. The potential sale of the oxygen by-product has not been taken into

account. It may contribute to increased revenues and thereby compensate for the high liquid hydrogen production cost. The high total capital investment and initial costs to start production might be a hindrance to implementing the proposed waste heat to hydrogen concepts. Subsidiary concepts like the Norwegian Enova programme, which supports investments in measures, which directly or indirectly contribute to reduction of carbon and greenhouse gas emissions, could be of help.

Despite the high initial costs, the studied concepts for waste heat recovery to hydrogen production present an interesting scheme for other municipal waste incineration based combined heat and power plants, which provide process and/or district heat only for a certain time of the year. As electricity prices are higher in many other European countries compared with Norway [47], for example, the proposed concepts for hydrogen production based on waste heat recovery could be an interesting option to use the available energy in waste more efficiently and reduce the amount of thermal energy rejected to the surroundings and the temperature it is rejected at. The rate of waste heat rejection to the surroundings could be reduced by ca. 30% in the investigated cases.

5 Conclusions

When waste heat cannot be sold as district heat by a combined heat and power plant, production of hydrogen by PEM electrolysis with power recovered from this low temperature waste heat can be economically feasible. The necessary condition is that the amount of available waste heat leads to an average cost of electricity lower than the cost of auxiliary electric power. In the studied case, compressed hydrogen at 350 bar can be produced at typical costs, while liquefying the hydrogen makes it too expensive compared with current prizes for liquid hydrogen from other sources. Although R1233zd(E) as ORC working fluid leads to a smaller annual production in the studied case, the lower capital costs lead to production costs similar to the use of ethanol as ORC working fluid. Even with the smallest calculated annual production of 251 tonne hydrogen, the waste management operator could reduce the amount and temperature of waste heat rejection from the CHP facility considerably; providing automotive fuel for its whole fleet of waste collection vehicles and at least 47 busses. A considerable reduction of local emissions from transport could be achieved because both public service vehicle (PSV) and refuse collection fleets are currently mainly Diesel powered.

Acknowledgements

The authors are grateful to BIR Avfallsenergi AS for information about waste collection and the waste incineration plant in Bergen, Norway. The authors are thankful to Gerard Ayuso Virgili from the Department of Biomedical Laboratory Sciences and Chemical Engineering at Western Norway University of Applied Sciences for help with the Aspen process simulation software. The authors are also thankful to Richard J. Grant from the Department of Mechanical and Marine Engineering at Western Norway University of Applied Sciences for giving the final manuscript a thorough language and grammar check. Assma Karouach and Stine Tveitan were bachelor students in the energy technology study programme at Western Norway University of Applied Sciences, campus Bergen.

Literature

[1] Office of the Prime Minister. A new and more ambitious climate policy for Norway. Available at: https://www.regjeringen.no/en/aktuelt/ny-og-mer-ambisios-klimapolitikk/id2393609/, accessed online: 10th august 2017.

[2] Statistics Norway. Emissions of greenhouse gases. Available at: https://www.ssb.no/en/natur-og-miljo/statistikker/klimagassn/aar-endelige, accessed online: 28th May 2018.

[3] İ. Yılmaz, M. İlbaş, M. Taştan, C. Tarhan. Investigation of hydrogen usage in aviation industry. Energy Conversion and Management. 63 (2012) 63-9.

[4] T. Solheimslid, H.K. Harneshaug, N. Lümmen. Calculation of first-law and second-law-efficiency of a Norwegian combined heat and power facility driven by municipal waste incineration – A case study. Energy Conversion and Management. 95 (2015) 149-59.

[5] Ø. Underdahl Holm (BIR AS), Properties of certain states in the steam cycles at the Rådal MSWI-plant. Personal Communication: January 2018, oyvind.holm@bir.no.

[6] C. Yilmaz, M. Kanoglu, A. Abusoglu. Exergetic cost evaluation of hydrogen production powered by combined flash-binary geothermal power plant. International Journal of Hydrogen Energy. 40 (2015) 14021-30.

[7] J. Sigurvinsson, C. Mansilla, B. Arnason, A. Bontemps, A. Maréchal, T.I. Sigfusson, et al. Heat transfer problems for the production of hydrogen from geothermal energy. Energy Conversion and Management. 47 (2006) 3543-51.

[8] C. Yilmaz, M. Kanoglu. Thermodynamic evaluation of geothermal energy powered hydrogen production by PEM water electrolysis. Energy. 69 (2014) 592-602.

[9] C. Yilmaz, M. Kanoglu, A. Abusoglu. Thermoeconomic cost evaluation of hydrogen production driven by binary geothermal power plant. Geothermics. 57 (2015) 18-25.

[10] I. Dincer, C. Acar. Review and evaluation of hydrogen production methods for better sustainability. International Journal of Hydrogen Energy. 40 (2015) 11094-111.

[11] H. Nami, F. Mohammadkhani, F. Ranjbar. Utilization of waste heat from GTMHR for hydrogen generation via combination of organic Rankine cycles and PEM electrolysis. Energy Conversion and Management. 127 (2016) 589-98.

[12] M.S. Shahin, M.F. Orhan, F. Uygul. Thermodynamic analysis of parabolic trough and heliostat field solar collectors integrated with a Rankine cycle for cogeneration of electricity and heat. Solar Energy. 136 (2016) 183-96.

[13] Y.E. Yüksel. Thermodynamic assessment of modified Organic Rankine Cycle integrated with parabolic trough collector for hydrogen production. International Journal of Hydrogen Energy. 43 (2018) 5832-41.

[14] D. Ferrero, M. Santarelli. Investigation of a novel concept for hydrogen production by PEM water electrolysis integrated with multi-junction solar cells. Energy Conversion and Management. 148 (2017) 16-29.

[15] L. Cao, J. Lou, J. Wang, Y. Dai. Exergy analysis and optimization of a combined cooling and power system driven by geothermal energy for ice-making and hydrogen production. Energy Conversion and Management. 174 (2018) 886-96.

[16] O. Schmidt, A. Gambhir, I. Staffell, A. Hawkes, J. Nelson, S. Few. Future cost and performance of water electrolysis: An expert elicitation study. International Journal of Hydrogen Energy. 42 (2017) 30470-92.

[17] N. Lümmen, E. Nygård, P.E. Koch, L.M. Nerheim. Comparison of organic Rankine cycle concepts for recovering waste heat in a hybrid powertain on a fast passenger ferry. Energy Conversion and Management. 163 (2018) 371-83.

[18] L. Branchini, A. De Pascale, A. Peretto. Systematic comparison of ORC configurations by means of comprehensive performance indexes. Applied Thermal Engineering. 61 (2013) 129-40.

[19] V. Chintala, S. Kumar, J.K. Pandey. A technical review on waste heat recovery from compression ignition engines using organic Rankine cycle. Renewable and Sustainable Energy Reviews. 81 (2018) 493-509.

[20] American Society of Heating Refrigerating and Air-Conditioning Engineers Inc. (ASHRAE). Designation and Safety Classification of Refrigerants. American Society of Heating, Refrigerating and Air-Conditioning Engineers, Inc. (ASHRAE), Atlanta, GA, USA, 2010.

[21] The European Parliament and the Council of the European Union. Regulation (EU) No 517/2014 on fluorinated greenhouse gases and repealing Regulation (EC) No 842/2006. The European Parliament and the Council of the European Union, Strasbourg. 2014.

[22] C. Yilmaz. Thermoeconomic modeling and optimization of a hydrogen production system using geothermal energy. Geothermics. 65 (2017) 32-43.

[23] M. Ni, M.K.H. Leung, D.Y.C. Leung. Energy and exergy analysis of hydrogen production by a proton exchange membrane (PEM) electrolyzer plant. Energy Conversion and Management. 49 (2008) 2748-56.

[24] T. Oi, K. Wada. Feasibility study on hydrogen refueling infrastructure for fuel cell vehicles using the off-peak power in Japan. International Journal of Hydrogen Energy. 29 (2004) 347-54.

[25] M.F. Renkel, N. Lümmen. Supplying hydrogen vehicles and ferries in Western Norway with locally produced hydrogen from municipal solid waste. International Journal of Hydrogen Energy. 43 (2018) 2585-600.

[26] B.J. McBride, S. Gordon, M.A. Reno. Coefficients for Calculating Thermodynamic and Transport Properties of Individual Species. NASA (National Aeronautics and Space Administration). Report no. 4513, 1993.

[27] O.K. Kjølstad, K.E. Vik. Mulighetsstudium for renovasjonsbiler på strøm og hydrogen. COWI,, Oslo, Norway. 2015. Retrieved from http://oreec.no/app/uploads/sites/2/a063847_prosjektrapport_mulighetsstudium-renovasjonsbiler-pa-strom-og-hydrogen_endelig-versjon-2.pdf, accessed online: 26th June 2018.

[28] I.H. Bell, J. Wronski, S. Quoilin, V. Lemort. Pure and Pseudo-pure Fluid Thermophysical Property Evaluation and the Open-Source Thermophysical Property Library CoolProp. Industrial & Engineering Chemistry Research. 53 (2014) 2498-508.

[29] A. Hammad, I. Dincer. Analysis and assessment of an advanced hydrogen liquefaction system. International Journal of Hydrogen Energy. 43 (2018) 1139-51.

[30] M.J. Moran, H.N. Shapiro, D.D. Boettner, M.B. Bailey. Principles of Engineering Thermodynamics. 8th ed. Wiley2015.

[31] C. Uysal, H. Kurt, H.-Y. Kwak. Exergetic and thermoeconomic analyses of a coal-fired power plant. International Journal of Thermal Sciences. 117 (2017) 106-20.

[32] A. Lazzaretto, G. Tsatsaronis. SPECO: A systematic and general methodology for calculating efficiencies and costs in thermal systems. Energy. 31 (2006) 1257-89.

[33] A. Bejan, G. Tsatsaronis, M. Moran. Thermal Design & Optimization. John Wiley & Sons, Inc., New York, USA, 1996.

[34] J. Xiong, H. Zhao, C. Zhang, C. Zheng, P.B. Luh. Thermoeconomic operation optimization of a coal-fired power plant. Energy. 42 (2012) 486-96.

[35] T. Igesund (BIR AS), Cost of waste transport to the Rådal MSWI-plant. Personal Communication: January 2019, toralf.igesund@bir.no.

[36] Directorate of Norwegian Customs. Exchange rates. Available at: https://www.toll.no/en/services/exchange-rates/, accessed online: 18th April 2018.

[37] H.K. Harneshaug, T. Solheimslid. Calculation of second law efficiency of energy recovery from waste [bachelor thesis]. Bergen, Norway: Bergen University College; 2014.

[38] T. Smolinka, M. Günther, J. Garche. Stand und Entwicklungspotenzial der Wasserelektrolyse zur Herstellung von Wasserstoff aus regenerativen Energien. Nationale Organisation Wasserstoff- und Brennstoffzellentechnologie GmbH, Berlin, Germany. 2010. Retrieved from https://www.now-gmbh.de/de/bundesfoerderung-wasserstoff-und-brennstoffzelle/projektfinder/wasserstoffbereitstellung/studie-wasserelektrolyse, accessed online: 6th June 2018.

[39] X-Rates. Historic Lookup. Available at: https://www.x-rates.com/historical/?from=USD&amount=1, accessed online: 26th June 2018.

[40] S.M. Saba, M. Müller, M. Robinius, D. Stolten. The investment costs of electrolysis – A comparison of cost studies from the past 30 years. International Journal of Hydrogen Energy. 43 (2018) 1209-23.

[41] K. Hellebust, M. Nord Flote. Offshore hydrogen production from wave energy [bachelor thesis]. Bergen, Norway: Western Norway University of Applied Sciences; 2018.

[42] A. Elgowainy, M. Mintz, J. Gillette, M. Ringer, B. Kelly, M. Hooks, et al. Hydrogen Delivery Analysis Models. U.S. Department of Energy. 2007. Retrieved from https://www.energy.gov/sites/prod/files/2014/03/f11/pipeline_group_paster_ms.pdf, accessed online: 27th May 2018.

[43] D. Mikielewicz, J. Mikielewicz. Analytical method for calculation of heat source temperature drop for the Organic Rankine Cycle application. Applied Thermal Engineering. 63 (2014) 541-50.

[44] BIR Transport AS. BIR Transport AS. Available at: https://bir.no/om-bir/%C3%A5rsrapport-2017/lovpaalagte-renovasjonstjenester/bir-transport-as/, accessed online: 26th June 2018.

[45] Norsk Hydrogenforum. Frequently asked questions. Available at: https://www.hydrogen.no/ressurser/ofte-stilte-sporsmal, accessed online: 26th June 2018.

[46] U.S. Drive Partnership. Hydrogen Production Tech Team Roadmap. 2017. Retrieved from https://www.energy.gov/sites/prod/files/2017/11/f46/HPTT%20Roadmap%20FY17%20Final_Nov%202017.pdf, accessed online: 26th July 2018.

[47] Eurostat. Electricity price statistics Available at: http://ec.europa.eu/eurostat/statistics-explained/index.php/Electricity_price_statistics, accessed online: 26th July 2018.